Theory of length-scale dependent relaxation moduli and stress fluctuations in glass-forming and viscoelastic liquids

L. Klochko, J. Baschnagel, J. Wittmer, H. Meyer, O. Benzerara, Alexander Semenov

▶ **To cite this version:**

L. Klochko, J. Baschnagel, J. Wittmer, H. Meyer, O. Benzerara, et al.. Theory of length-scale dependent relaxation moduli and stress fluctuations in glass-forming and viscoelastic liquids. The Journal of Chemical Physics, 2022, 156 (16), pp.164505. 10.1063/5.0085800 . hal-03806940

HAL Id: hal-03806940
https://hal.science/hal-03806940v1

Submitted on 8 Oct 2022

HAL is a multi-disciplinary open access archive for the deposit and dissemination of scientific research documents, whether they are published or not. The documents may come from teaching and research institutions in France or abroad, or from public or private research centers.

L'archive ouverte pluridisciplinaire **HAL**, est destinée au dépôt et à la diffusion de documents scientifiques de niveau recherche, publiés ou non, émanant des établissements d'enseignement et de recherche français ou étrangers, des laboratoires publics ou privés.

Theory of length-scale dependent relaxation moduli and stress fluctuations in glass-forming and viscoelastic liquids

L.Klochko, J.Baschnagel, J.P.Wittmer, H.Meyer, O.Benzerara, A.N.Semenov[a)1]

Institut Charles Sadron, CNRS - UPR 22, Université de Strasbourg, 23 rue du Loess, BP 84047, 67034 Strasbourg Cedex 2, France

(Dated: 5 April 2022)

The spacio-temporal correlations of the local stress tensor in supercooled liquids are studied both theoretically and by MD simulations of a two-dimensional (2D) polydisperse Lennard-Jones system. Asymptotically exact theoretical equations defining the dynamical structure factor and all components of the stress correlation tensor for low wave-vector q are presented in terms of the generalized (q-dependent) shear and longitudinal relaxation moduli, $G(q,t)$ and $K(q,t)$. We developed a rigorous approach (valid for low q) to calculate $K(q,t)$ in terms of certain bulk correlation functions (for $q=0$), the static structure factor $S(q)$ and thermal conductivity κ. The proposed approach takes into account both the thermostatting effect and the effect of polydispersity. The theoretical results for the (q,t)-dependent stress correlation functions are compared with our simulation data, and an excellent agreement is found for $q\bar{b} \lesssim 0.5$ (with $\bar{b}$, the mean particle diameter) both above and below the glass transition without any fitting parameters. Our data are consistent with recently predicted (both theoretically and by simulations) long-range correlations of the shear stress quenched in heterogeneous glassy structures.

[a)] Author to whom correspondence should be addressed: al.ni.semenov@gmail.com

I. INTRODUCTION

Mechanical stress governs the flow and deformation dynamics in liquids or amorphous solids (glasses).[1,2] The stress correlation functions therefore provide important information on dynamical properties of amorphous materials.[3] In particular, it is well-known that time-dependent correlations of the shear stress $\sigma(t)$ are related to the shear relaxation modulus, $G(t)$,[4–10] which is one of the central rheological functions of a material:

$$\left\langle \sigma(t+t')\sigma(t') \right\rangle = \frac{T}{V} G(t) + \text{const} \tag{1}$$

where V is the system volume and T is its temperature in energy units ($T = k_B T_{abs}$ where T_{abs} is the standard absolute temperature), and 'const' is a constant[5,6,9,10,12] that vanishes in an equilibrium liquid, but may take a non-zero value for systems with finite (quasi-) static shear modulus. A similar relation between the correlation function, $C_p(t)$, of instantaneous pressure $p(t)$, and the bulk compression modulus $K_0(t)$ was recently discussed[10] (see also Refs. 7, 8, 16, and 17). $K_0(t)$ defines the pressure response after a small uniform compression of the system volume ($V \to V(1-\varepsilon)$, $\varepsilon \ll 1$) at $t = 0$:

$$\Delta p(t) = \varepsilon K_0(t),\ t > 0 \tag{2}$$

In addition to $K_0(t)$, there are two other response functions related to compression and useful for many purposes[10]: (i) The adiabatic compression modulus $K_A(t)$ characterizes a thermally isolated system whose energy and entropy are constant at $t > 0$ (no heat exchange with its environment). (ii) The isothermal compression modulus $K_T(t)$ is relevant to the ideal case when the system temperature is kept perfectly constant. These two functions characterize the system as such, whereas the pressure correlation function $C_p(t)$ depends also on the thermostatting conditions, and so it is non-universal in this respect (see note[62]).

In particular, such dependence on the thermostatting mechanism applies to most of molecular dynamics (MD) simulation studies.[10] This effect is akin to the well-known fact that static correlators (like $C_p(0)$) generally depend on the statistical ensemble.[18] It is possible, however, to obtain the universal (thermostat-independent) material functions, $K_A(t)$ and $K_T(t)$, based on cross- and auto-correlation functions of pressure and temperature. Some recipes on how to do it are described in Ref. 10 (see also Ref. 11).

Complex and glass-forming liquids are known to be highly heterogeneous[19], so the space-resolved correlation functions are required to characterize their structure. Accordingly, in the

present paper we study the stress correlation and response functions depending on both wave-vector ($\underline{q}$) and time (t). In particular, we consider all components of the tensorial correlation function $C_{\alpha\beta\alpha'\beta'}(\underline{q},t)$ (defined in eq. 69) for the q-dependent stress, $\sigma_{\alpha\beta}(\underline{q},t)$. The latter is the Fourier transform of the stress tensor field $\sigma_{\alpha\beta}(\underline{r},t)$:

$$\sigma_{\alpha\beta}(\underline{q},t) = (1/V)\int \sigma_{\alpha\beta}(\underline{r},t)\exp(-\mathrm{i}\underline{q}\cdot\underline{r})\mathrm{d}^d r \tag{3}$$

where α,β refer to Cartesian components and d is the space dimension. To simplify the analysis we consider here only strictly two-dimensional systems (2D, $d=2$), although many results obtained below are more general. The stress correlation functions are first predicted theoretically (see section III B), and then the results are compared with our MD simulation data (section III C) on a 2-dimensional polydisperse Lennard-Jones (pLJ) system described in Appendix A.

The theory of time-space resolved stress correlations was developed in several recent studies using either the Zwanzig-Mori projection operator formalism[14,20,21] or the fluctuation-dissipation theorem (FDT)[6]. Both approaches considered isothermal systems (formally assuming infinite thermal conductivity) and eventually specify the theories in the hydrodynamic limit of small q (in 2D in Ref. 6, and in arbitrary dimension d in Refs. 20 and 21). The results for the stress correlation tensor obtained within these theories are in harmony with each other. In particular, both theories predict a long-range power law tail ($1/r^d$) for long-time shear stress correlations, $C_{xyxy}(\underline{r},t)$, for supercooled viscoelastic liquids and amorphous systems below the glass-transition temperature. This prediction is in qualitative agreement with simulation data on stress correlations in 2D[22] and 3D binary LJ models[23]. Recent theoretical, experimental and simulation studies of static strain correlations in 2D colloidal glass-formers reveal an Eshelby-strain pattern with a characteristic $1/r^2$ long-range decay near the glass transition.[58] A similar $1/r^3$ decay for strain correlations has been also predicted and tested against simulations and experiments on 3D Brownian hard-sphere colloids[15]. However, to the best of our knowledge, a full quantitative comparison of theoretical and simulation results on $\underline{q},t$-resolved stress correlations has not been performed yet. Here we present such a comparison in 2D. In doing so, we also extend the previous theory[6] by including the effects due to heat transport and particle-size polydispersity, both of which are important for a quantitative analysis of the stress correlation tensor for the simulated glass-forming system.

In the next section we introduce the generalized q,t-dependent longitudinal modulus $K(q,t)$ and argue that for $q \neq 0$ it is essentially universal (independent of the ensemble/thermostat) in contrast to $K(0,t)$ and various correlation functions of volume-averaged quantities (section II C).

A theoretical approach allowing to obtain $K(q,t)$ based on standard time-dependent correlation functions (at $q=0$) is presented as well. We then describe a recipe for efficient numerical calculation of $K(q,t)$ taking into account both heat conduction and polydispersity of a molecular or colloidal system (see sections II D, II E, II F), and finally obtain the longitudinal response function for the (2D pLJ) model Lennard-Jones system defined in Appendix A. In the 3rd section it is first explained how to obtain the dynamical structure factor $S(q,t)$ based on $K(q,t)$; the theoretical approach is then verified by comparison with the simulation data for the 2D pLJ model. Furthermore, in section III B we present the basic relations (mostly coming from the FDT) defining the stress-correlation tensor $C_{\alpha\beta\alpha'\beta'}(\underline{q},t)$ in terms of the generalized shear ($G(q,t)$) and longitudinal ($K(q,t)$) moduli. All independent components of the stress-correlation tensor are then calculated numerically as described therein. The theoretical and simulation results for $C_{\alpha\beta\alpha'\beta'}(\underline{q},t)$ are compared in section III C followed by a further discussion of the generalized elastic moduli in section IV revealing long-range spacio-temporal stress correlations. The main results are summarized in section V. Finally, Appendix B describes the theory for the temperature autocorrelation function used to determine the thermal conductivity κ.

II. THE Q-DEPENDENT RELAXATION MODULI

A. Uniform deformations, $q=0$

In the present study we are mostly interested in two relaxation moduli, $G(q,t)$ and $K(q,t)$ corresponding to shear and longitudinal deformation, respectively.[4,24,25,27] Their definition for $q=0$ is well-known: $G(0,t)\equiv G(t)$ is the classical shear relaxation modulus related to the (ensemble-averaged) shear stress response, $\Delta\sigma_{xy}(t)$, upon a canonical-affine xy-shear deformation γ when the coordinates ($\underline{r}$) and velocities ($\underline{v}$) of all particles are instantly changed at $t=0$ as

$$r_y \to r_y + \gamma r_x, \quad v_x \to v_x - \gamma v_y \tag{4}$$

(for shear along y-axis with gradient in x-direction):

$$\Delta\sigma_{xy}(t) = G(t)\gamma \tag{5}$$

for $\gamma \to 0$. $G(t)$ is therefore the linear response function (quadratic and higher-order terms in γ and other perturbation magnitudes are neglected here and in what follows).

The longitudinal modulus $K(0,t) \equiv K_L(t)$ is defined in a similar way as a response of longitudinal pressure, $p_{xx} = -\sigma_{xx}$, to a small uniaxial compression $\varepsilon = -\varepsilon_{xx}$ of the system at $t = 0$ (while the transverse area, i.e. the cross-section perpendicular to the deformation axis, is kept constant),

$$r_x \to r_x(1-\varepsilon), \quad v_x \to v_x(1+\varepsilon) \tag{6}$$

The ensemble-averaged longitudinal pressure increment is then

$$\Delta p_{xx}(t) = K_L(t)\varepsilon \tag{7}$$

It is well-known that in isotropic systems the two moduli fully define the stress response to any affine deformation[28,29]. In particular, eq. 7, can be supplemented with

$$\Delta p_{yy}(t) = M(t)\varepsilon$$

where $M(t) = K_L(t) - 2G(t)$ is the transverse modulus. The bulk compression modulus $K_0(t)$ (cf. Ref. 10) is therefore related to K_L:

$$K_L(t) = K_0(t) + (2 - 2/d)G(t) \tag{8}$$

where d is the space dimension.

The moduli $G(t)$ and $M(t)$ can be thought of as time-dependent generalizations of the elastic coefficients of isotropic solids[28,29]: $G(t)$ corresponds to the shear modulus μ and $M(t)$ to the Lamé coefficient λ. With this correspondence the longitudinal modulus $K_L(t) = M(t) + 2G(t)$ agrees with the known relation from the linear elasticity ($K_L = \lambda + 2\mu$) and the bulk compression modulus $K_0(t)$ with that for the classical static bulk modulus ($K_0 = \lambda + 2\mu/d$).

B. Non-uniform deformations, $q \neq 0$

In this section we formulate a microscopic definition of the generalized q-dependent relaxation moduli (which is alternative to the usually adopted way to define them based on phenomenological hydrodynamic equations[3,24]).

It is well-known that in the general case the deformation rate is defined by the flow velocity field $\underline{v}(\underline{r},t)$.[31] The microscopic definition of its Fourier transform, $\underline{v}(\underline{q},t) = V^{-1}\int \underline{v}(\underline{r},t)\exp\left(-\mathrm{i}\underline{q}\cdot\underline{r}\right)\mathrm{d}^d r$, is:

$$\underline{v}(\underline{q},t) = \underline{J}(\underline{q},t)/\rho \tag{9}$$

where $\rho = \sum_a m_a/V$ is mean mass density, $\underline{J}$ is momentum density,

$$\underline{J}(\underline{q},t) = V^{-1}\sum_a m_a \underline{v}_a(t)\exp\left(-\mathrm{i}\underline{q}\cdot\underline{r}_a(t)\right) \tag{10}$$

$a = 1,\ldots,N$ is the label of a particle, and m_a, $\underline{v}_a$ and $\underline{r}_a$ are the mass, velocity and position of the a-th particle, respectively. The deformation rate is related to the tensor of velocity gradients

$$\dot{\gamma}_{\alpha\beta} = \frac{\partial v_\beta(\underline{r},t)}{\partial r_\alpha} = \sum_{\underline{q}} \mathrm{i}q_\alpha v_\beta(\underline{q},t)\exp\left(\mathrm{i}\underline{q}\cdot\underline{r}\right) \tag{11}$$

where the sum runs over all $\underline{q}$-modes defined by the system size, and α, β are Cartesian components. Here we assume that the system boundaries are fixed (undeformed),[13] and that is why there is no deformation at $q = 0$.

Let us consider a single deformation mode with $q \neq 0$. Without loss of generality we can assume that $\underline{q}$ is parallel to the x-axis. Then $\dot{\gamma}_{xy} = \dot{\gamma}e^{\mathrm{i}qx}$ (with $\dot{\gamma} = \mathrm{i}qv_y$) is the generalized shear deformation rate, and $\dot{\varepsilon}_{xx} = -\dot{\varepsilon}e^{\mathrm{i}qx}$ with $\dot{\varepsilon} = -\mathrm{i}qv_x$ correspond to the generalized longitudinal deformation. An instant shear deformation mode with amplitude γ is emerged at $t = 0$ if $\dot{\gamma} = \gamma\delta(t)$ is imposed by means of an external force field; this deformation is equivalent to imposing $v_y = -\mathrm{i}\gamma\delta(t)/q$, where δ is the Dirac's δ-function. Similarly, an instant external longitudinal deformation with amplitude ε corresponds to $v_x = \mathrm{i}\varepsilon\delta(t)/q$. The resultant particle displacement field is

$$\underline{u}(\underline{r}) = \frac{\mathrm{i}}{q}\left(\varepsilon\hat{x} - \gamma\hat{y}\right)e^{\mathrm{i}qx} \tag{12}$$

where $\hat{x}$ is the unit vector along the x-axis and $\hat{y}$ along the y-axis. To render the whole deformation canonical the particle velocities should be changed accordingly (cf. eqs. 4, 6):

$$\underline{v} \to \underline{v} + \hat{x}e^{\mathrm{i}qx}\left(\varepsilon v_x - \gamma v_y\right) \tag{13}$$

Note that at $q = 0$ the above equation agrees with eqs. 4, 6.

The generalized moduli can then be defined via the ensemble-averaged stress responses to the specified instant shear and longitudinal deformations at a wave-vector $\underline{q}$:

$$\Delta\sigma_{xy}(\underline{q},t) = G(\underline{q},t)\gamma, \;\; \Delta p_{xx}(\underline{q},t) = K(\underline{q},t)\varepsilon \tag{14}$$

The above equations are valid provided that no further deformation occurs at $t > 0$:

$$\underline{J}(\underline{q},t) \equiv 0 \text{ at } t > 0 \tag{15}$$

However, the very stress generated by the initial deformation at $t = 0$ would lead to a flow giving rise to further deformations of the system. This flow is governed by the fundamental momentum equation[3,6]

$$\frac{\partial J_\alpha(\underline{q},t)}{\partial t} = \mathrm{i} q_\beta \sigma_{\alpha\beta}(\underline{q},t) \tag{16}$$

Therefore, in the general case the stress response comes as a linear superposition of contributions from all the previous small deformations. So, for example, the first eq. 14 should be replaced by[31]

$$\Delta\sigma_{xy}(\underline{q},t) = G(\underline{q},t)\gamma(0) + \int_{0^+}^{t} G(\underline{q},t-t')\mathrm{d}\gamma(t') \tag{17}$$

where $\mathrm{d}\gamma(t')/\mathrm{d}t'$ is the deformation rate defined by $\underline{v}(\underline{q},t)$. To avoid this complication, one can apply a perturbative external force $\underline{F}(\underline{q},t)$ to the system (adding it to the rhs of eq. 16) in order to prevent any deformation at $t > 0$ (that is, to render eq. 15 valid at all times after the initial deformation). In real space this is equivalent to application of an external force field with

$$\underline{F}_a(t) = m_a \underline{A}(t) e^{\mathrm{i}\underline{q}\cdot\underline{r}_a} \tag{18}$$

being the force on the a-th particle. Here $\underline{A}(t)$ is proportional to $\underline{F}(\underline{q},t)$. (Indeed, recalling the definition of the Fourier transform we get $\underline{F}(\underline{q},t) = \frac{1}{V}\sum_a \underline{F}_a(t) e^{-\mathrm{i}\underline{q}\cdot\underline{r}_a} = \rho\underline{A}(t)$). Obviously, the forces $\underline{F}_a(t)$ provide a coherent acceleration of all particles (with amplitude $\underline{A}(t)$).[26]

Since physical variables like $\underline{r}_a(t)$, $\underline{v}_a(t)$ are necessarily real, changing $\underline{q}$ to $-\underline{q}$ always leads to complex conjugation of $\underline{q}$-dependent variables. Hence, for example, $\sigma_{\alpha\beta}(-\underline{q},t) = \sigma^*_{\alpha\beta}(\underline{q},t)$ (cf. eq. 3). Therefrom we get $G^*(\underline{q},t) = G(-\underline{q},t)$, $K^*(\underline{q},t) = K(-\underline{q},t)$. Besides, the isotropy of the system also ensures that these response functions depend only on $|q|$, hence they must be real.

C. Low-q regime for $G(q,t)$ and $K(q,t)$

Having defined the generalized relaxation moduli, we now turn to the problem of their calculation. $G(q,t)$ at $q = 0$ is a central rheological function, and there are well-known techniques to obtain it either experimentally[31] or based on simulation data.[4,5,7–10,32] A commonly employed efficient way to calculate $G(t)$ is to use eq. 1. As for the q-dependence of G, we stick to the idea that $G(q,t)$ is uniformly continuous at $q \to 0$[3,6,20], hence the following approximation is reasonable:

$$G(q,t) \simeq G(t) \text{ for } \lambda \gg \bar{b} \tag{19}$$

where $\lambda = 2\pi/q$ is the wavelength, and $\bar{b}$ is the molecular size (i.e., the mean particle diameter for the pLJ system we consider). Moreover, we are confident that the q-dependence of G is regular,

so the deviation of $G(q,t)$ from $G(t)$ is proportional to q^2. For molecular systems with finite interaction range this can be rigorously proved for $t = 0$ (details to be given elsewhere). For $t > 0$ a weak q-dependence of $G(q,t)$ at low q's comes from the following physical argument: let's divide the system in cells of size l, $\bar{b} \ll l \ll \lambda$; within each cell the deformation is almost uniform, so the stress response is nearly given by $G(t)$; any effect of stress relaxation in a distant cell cannot be transferred to a given cell because any deformation (at $t > 0$) is forbidden by definition of $G(q,t)$, so there is no mechanism by which a structural relaxation of a given cell can be coupled with that in a distant cell (the locality principle).

It may seem that the above argument is also applicable to the longitudinal modulus $K(q,t)$, which would imply the relation $K(q,t) \simeq K(q=0,t) = K_L(t)$. However, this approximation does not hold. On the one hand, it is well known that fluctuations of volume-averaged (i.e., $q = 0$) variables, like longitudinal stress $\sigma_{xx}(t)$ or pressure $p(t)$, depend on the statistical ensemble[27,32]. On the other hand, the related moduli $K_L(t)$ and $K_0(t)$ also depend on whether the dynamics is energy-conserving or thermostatted and thus, in the latter case, on the nature and parameters of the thermostat used in the simulation.[10] This is so because a compression of the system leads to a temperature rise whose evolution is controlled by the thermostat, and thus entails a thermostat-dependent pressure response.[10] By contrast, the longitudinal modulus $K(q,t)$ for $q > 0$ is universal: it does not depend on the statistical ensemble or the presence of a thermostat. The main reason for this is that fluctuations of physical fields at $q > 0$ are not coupled with volume-averaged (i.e., $q = 0$) fluctuations of the mean T which are controlled by the thermostat. Therefore, $\lim_{q\to 0} K(q,t)$ is universal, while $K(q=0,t) = K_L(t)$ is not. As a result, $K(q,t)$ can be discontinuous at $q = 0$.[30] Noteworthily, the effects considered just above are not relevant for $G(t)$ since the shear stress σ_{xy} is not coupled with any scalar field (in particular, temperature fluctuations) for symmetry reasons. Hence, it does not matter for $G(t)$ whether the dynamics is energy-conserving or thermostatted.

To sum up, $G(q,t)$ just weakly (negligibly in the regime $q\bar{b} \ll 1$) depends on q because the local shear stress response to a prescribed shear deformation depends on the local structure only. By contrast, the longitudinal stress response to a small inhomogeneous extension ε (at a small wave-vector q) can significantly depend on q since such a response (associated with $K(q,t)$) depends not only on the deformation ε, but also on the deformation-induced temperature (T) increment which is (essentially) a slow conserved variable whose relaxation dynamics is non-local. As a result $K(q,t)$ gets non-local dynamically, i.e., at $t > 0$, due to the stress-temperature coupling (by contrast $K(q,t=0)$ can be approximated by its $q \to 0$ limit just like $G(q,t)$).

D. Calculation of $K(q,t)$ for monodisperse systems

In the previous section we showed that a relation like eq. 19 does not work for the longitudinal modulus $K(q,t)$. Is it possible at all to find $K(q,t)$ based on correlation functions at $q=0$? The answer is positive, but the problem is not exactly trivial as clarified below.

Recently[10] we showed how to obtain two universal bulk compression relaxation moduli, $K_A(t)$ for adiabatic compression and $K_T(t)$ for isothermic compression, based on correlation data from thermostatted simulations. We also described how to calculate two other universal functions: the time dependent isochoric heat capacity per particle, $c_v(t)$, and the thermal pressure $p_T(t)$.[10,11] The latter function is defined via the isochoric pressure response (at constant volume), $\Delta p(t)$, to an instant small temperature rise, ΔT, at $t=0$:

$$\Delta p(t) = p_T(t)\Delta T \tag{20}$$

Its static limit is a thermodynamic derivative: $p_T(\infty) = (\partial p/\partial T)_V$. As shown below, $K(q,t)$ at low q can be expressed in terms of these functions. The result also depends on the thermal conductivity κ of the system. If $\kappa = 0$, there is no heat transfer, so $K(q,t)$ must be nearly equal to the adiabatic longitudinal modulus $K_{AL}(t)$ (here we apply the same locality principle as for $G(q,t)$):

$$K(q,t) \simeq K_{AL}(t), \;\; \lambda \equiv 2\pi/q \gg \bar{b} \tag{21}$$

where

$$K_{AL}(t) = K_A(t) + (2-2/d)G(t) \tag{22}$$

by virtue of eq. 8.

In the general case (finite κ) the modulus $K(q,t)$ is lower. To obtain it we note that in addition to the adiabatic deformation of a cell applied at $t=0$ (with compression strain $\varepsilon = -\varepsilon_{xx}$), some heat $h(t)$ can be transferred to it later on (at $t>0$) by thermal conduction. The heat itself leads to a pressure increment

$$\Delta p^{(h)}(t) = \int_{-\infty}^{t} \frac{\mathrm{d}h(t')}{\mathrm{d}t'} \chi(t-t')\mathrm{d}t' \tag{23}$$

where $\chi(t)$ is the relevant response function, and $h(t)$ is the heat (per particle) injected into the cell by the time t (the heat injected during a time-period between t and $t+\Delta t$ therefore equals $h(t+\Delta t) - h(t)$). Therefore, the total longitudinal pressure increment is

$$\Delta p_{xx}(t) = K_{AL}(t)\varepsilon + \Delta p^{(h)}(t) \tag{24}$$

where the first term in the rhs is due to adiabatic xx-compression, and the last term is the stress increment due to thermal conductivity leading to the energy increment $h(t)$. Here and below we assume for simplicity that the wave-vector $\underline{q}$ is oriented along the x-axis, so the x-dependence of pressure increment Δp_{xx} (and other variables: ΔT, h, ε) is given by the factor $e^{\mathrm{i}qx}$ which is systematically omitted. (Note that the heat-induced stress tensor change is $\Delta\sigma^{(h)}_{\alpha\beta}(t) = -\Delta p^{(h)}(t)\delta_{\alpha\beta}$ since energy is a scalar variable.)

In order to find $\chi(t)$ we note that the heat $h(t)$ leads to a temperature perturbation, $\Delta T^{(h)}(t)$, such that

$$h(t) = \int_{-\infty}^{t} c_v(t-t')\frac{\mathrm{d}}{\mathrm{d}t'}\Delta T^{(h)}(t')\mathrm{d}t' \tag{25}$$

where $c_v(t)$ is time-dependent isochoric heat capacity per particle. Eqs. 23, 25 can be simplified by using a modified Laplace transform[10,11] referred to in what follows as 's-transform' and defined for a function $X(t)$ as

$$X(t) \;\rightarrow\; X(s) = s\int_0^{\infty} X(t)e^{-st}\mathrm{d}t \tag{26}$$

Eqs. 23, 25, 20 then read in terms of s-transforms:

$$\Delta p^{(h)}(s) = h(s)\chi(s) \tag{27}$$

$$h(s) = c_v(s)\Delta T^{(h)}(s) \tag{28}$$

$$\Delta p^{(h)}(s) = p_T(s)\Delta T^{(h)}(s) \tag{29}$$

The above equations lead to

$$\chi(s) = p_T(s)/c_v(s) \tag{30}$$

and (cf. eq. 24)

$$\Delta p_{xx}(s) = K_{AL}(s)\varepsilon + h(s)p_T(s)/c_v(s) \tag{31}$$

It therefore remains to find $h(s)$. It is defined by the heat transport equation

$$n_0\frac{\partial h(t)}{\partial t} = \kappa\nabla^2 T = -\kappa q^2\Delta T \tag{32}$$

where $n_0 = N/V$ is the mean concentration, and the Laplacian ∇^2 is replaced with $-q^2$ in view of the harmonic dependence of all perturbations given by the factor $e^{\mathrm{i}\underline{q}\cdot\underline{r}}$. Here

$$\Delta T(t) = \Delta T^{(i)}(t) + \Delta T^{(h)}(t) \tag{33}$$

is the total temperature increment due to two effects: (i) initial instant adiabatic compression, $\varepsilon = -\varepsilon_{xx}$, at $t = 0$; (ii) the heat conduction. Applying the FDT to an energy-conserving canonical ensemble we get:

$$\Delta T^{(i)}(t) = \varepsilon \frac{T}{n_0} \chi(t) \tag{34}$$

(The latter equation can be obtained by using eqs. (B2), (B9) of Ref. 10 and noting that ΔT in eq. (B2) is actually $\Delta T^{(i)}$, and that the 2nd term in the 1st eq. (B9) represents $\Delta p^{(h)}$ with $h = \varepsilon_v T$.) Physically, eq. 34 comes from the fact that $\Delta p^{(h)}$ as predicted by the FDT is proportional to

$$C_{pT}(t) = \frac{N}{T^2} \left\langle \delta p(t+t') \delta T(t') \right\rangle \tag{35}$$

while $\Delta T^{(i)}$ must be proportional to $C_{Tp}(t)$ which is equal to $C_{pT}(t)$.[33] In the static limit, $t \to \infty$, eq. 34 simply comes from eq. 27 and the thermodynamic relation: $T\left(\partial p/\partial E\right)_V = -\left(\partial T/\partial V\right)_S$, where E, S are total energy and entropy, respectively.

As a result, using eqs. 28, 34 we get:

$$\Delta T(s) = \left[\varepsilon \frac{T}{n_0} p_T(s) + h(s) \right] / c_v(s) \tag{36}$$

Next, we use the above equation, eq. 31, and eq. 32 whose s-transform reads $sh(s) = -(\kappa/n_0) q^2 \Delta T(s)$, to obtain $\Delta p_{xx}(t) = K(q,t)\varepsilon$ with

$$K(q,s) = K_{AL}(s) - \frac{T}{n_0} \frac{p_T(s)^2}{c_v(s)} \left[1 + s n_0 c_v(s) / \left(\kappa q^2 \right) \right]^{-1} \tag{37}$$

We anticipate that this equation is valid at low q's with relative accuracy of $\sim (\bar{b}/\lambda)^2$ (cf. eq. 19 for $G(q,t)$). Still the sign ' =' is used here and below to simplify equations (whose approximate nature must be kept in mind). For $\kappa \to 0$ the 2nd term in the above equation vanishes, so the modulus $K(q,t)$ becomes purely adiabatic and eq. 21 is recovered. By contrast, for $\kappa \to \infty$ eq. 37 becomes

$$K(q,s) = K_{AL}(s) - \frac{T}{n_0} \frac{p_T(s)^2}{c_v(s)} \equiv K_{TL}(s) \tag{38}$$

In this case $K(q,t) = K_{TL}(t)$, where $K_{TL}(t) = K_T(t) + (2 - 2/d) G(t)$ is the isothermic longitudinal modulus defined in eq. 38. Note that the difference $K_{AL}(t) - K_{TL}(t)$ is equal to $K_A(t) - K_T(t)$ (cf. eq. (D23) of Ref. 10) as it should be. The general eq. 37 can be rewritten in terms of the isothermic relaxation modulus K_{TL}:

$$K(q,s) = K_{TL}(s) + T p_T(s)^2 / \left[n_0 c_v(s) + \kappa q^2 / s \right] \tag{39}$$

Finally, the relaxation modulus $K(q,t)$ can be obtained by doing an inverse s-transform of eq. 37 or eq. 39 provided that the response functions $K_{AL}(s)$, $p_T(s)$, $c_v(s)$ are known. A rigorous way to obtain these functions based on correlation data from thermostatted simulations was described recently[10,11]. Noteworthily, the approach to obtain the general relations between time and wave-vector dependent response functions and correlation functions developed here and in refs. 10 and 11 is similar to the generalized hydrodynamic theory[38,47]. The main differences are that (i) we now adapt the theory rendering it applicable to the thermostatted simulations with imperfect temperature control, so that the universal (thermostat independent) response functions can be calculated based on non-universal dynamical correlation functions, and (ii) we systematically use the s-transform (instead of merely the Laplace transform of time-dependent functions) which renders many dynamical relations between response functions look pretty similar to their static counterparts (see, e.g., eqs. (D23) and (D25) of ref. 10, or eq. 77 below).

In the next section we propose rather simple approximate ways to obtain $K(q,s)$ which largely avoid the need to do direct or inverse Laplace transforms.

E. Approximate relations for $K(q,t)$

In most thermostatted simulation schemes the isothermicity condition only holds at long enough time-scales, $t \gg \tau_{damp}$, where τ_{damp} is the characteristic damping time associated with the thermostat employed in the simulations. As a result, a simple linear relation between, say, the dynamical heat capacity, $c_v(t)$, and the energy autocorrelation function gets violated, so one has to resort to more complicated equations[10,11]. A simple way out is to set the thermostat parameters so as to decrease the characteristic time τ_{damp} below the time-scales of interest. We adopted this way in simulations of the 2D pLJ system involving the Nosé-Hoover thermostat (see Appendix A): the chosen thermostat-related Nosé time, $\tau_{damp} \sim 0.01$, ensured that $T \approx \text{const}$ at $t \gtrsim 0.1$, which means that all the correlation data (with the sampling time-step of $\delta t = 0.05$) are nearly isothermic, maybe except for $t = 0,\, 0.05$.[34] Then, all correlations involving temperature fluctuations can be neglected, and it is reasonable to approximate $c_v(t)$ with $c_{v0}(t) = C_E(0) - C_E(t)$,[35] $p_T(t)$ with $p_{T0}(t) = C_{pE}(0) - C_{pE}(t)$, and $K_T(t)$ with $K_0(t) = \frac{T}{n_0}\left[C_p(t) - C_p(0)\right] + \eta_A$, where (see Refs. 10 and 11 for details)

$$C_p(t) = \frac{N}{T^2}\left\langle \delta p(t+t')\delta p(t')\right\rangle \tag{40}$$

$$C_{pE}(t) = \frac{1}{T^2}\left\langle \delta p(t+t')\delta E(t')\right\rangle, \;\; C_E(t) = \frac{1}{T^2 N}\left\langle \delta E(t+t')\delta E(t')\right\rangle \tag{41}$$

Here E is the total energy of the system, $\eta_A = K_0(0)$ is its affine compression modulus, $\delta X(t) = X(t) - \langle X\rangle$, and $\langle X\rangle$ means time and ensemble average of a variable X. Applying these approximations in eq. 39 leads to

$$K(q,s) \simeq K_*(q,s) \equiv K_L(s) + T\,p_{T0}(s)^2 / \left[n_0 c_{v0}(s) + \kappa q^2/s\right] \tag{42}$$

where $K_L(s) = K_0(s) + (2-2/d)G(s)$. Using simulation data on the correlation functions for the system described in Appendix A we established that the approximation, eq. 42, works remarkably well: it is asymptotically exact both at short and long t, and at intermediate times its relative error is $\lesssim 0.1\%$, which is comparable to (or smaller than) the statistical error bar of our data.

Eq. 42 can be used to obtain the longitudinal modulus in the time domain:

$$K(q,t) \approx K_*(q,t) \equiv K_L(t) + \Delta K_*(q,t) \tag{43}$$

where the 1st term is $K_L(t) = K_0(t) + (2-2/d)G(t) \approx K_{TL}(t)$, and the s-transform of the 2nd term is

$$\Delta K_*(q,s) = \frac{T}{n_0}\frac{p_{T0}(s)^2}{\psi(s)}, \;\; \psi(s) \equiv c_{v0}(s) + \frac{\kappa}{n_0}q^2/s \tag{44}$$

It leads to the following equation for $\Delta K_*(q,t)$:

$$\int_0^t \Delta K_*(q,t-t')\mathrm{d}\psi(t') = \frac{T}{n_0}\int_0^t p_{T0}(t-t')\mathrm{d}p_{T0}(t') \tag{45}$$

where

$$\psi(t) = c_{v0}(t) + \frac{\kappa}{n_0}q^2 t \tag{46}$$

Eq. 45 is similar to eq. (D7) of Ref. 10 and can be solved numerically in the same way. The results for our 2D pLJ model system at $q = q_{\min} \equiv 2\pi/L$ (L is the system box size) and $T = 0.4,\ 0.3,\ 0.26,\ 0.24,\ 0.2$ are shown in Fig. 1 (black curves from bottom to top). The reduced thermal conductivity, $\kappa^* = \kappa q_{\min}^2/n_0 = (2\pi)^2\,\kappa/N$, was obtained based on temperature autocorrelation data as described in Appendix B: $\kappa^* = 0.0426,\ 0.0474,\ 0.0466,\ 0.0471,\ 0.0490$ for $T = 0.4,\ 0.3,\ 0.26,\ 0.24,\ 0.2$, respectively. It is apparent that κ increases just slightly as T is decreased.

A simple approximate expression for $\Delta K_*(q,t)$ can be obtained by assuming that p_{T0} and c_{v0} are constants, then doing analytically the inverse s-transform of eq. 44, and then replacing p_{T0} and

c_{v0} with time-dependent functions:

$$\Delta K_*(q,t) \approx \frac{T}{n_0}\frac{p_{T0}(t)^2}{c_{v0}(t)}\exp\left(-\frac{\kappa q^2 t}{n_0 c_{v0}(t)}\right) \tag{47}$$

This equation is analogous to eq. (A5) of Ref. 10. The above approximation of $\Delta K_*(q,t)$ was used to calculate $K(q,t) \approx K_L(t) + \Delta K_*(q,t)$. The results are also shown in Fig. 1 by red curves. One can observe that the approximation, eq. 47, works very well in a wide T-range (both above and below the glass transition temperature $T_g \approx 0.26$).[39] The relative error is $\lesssim 1\%$ for $T = 0.4,\ 0.3$ and $\lesssim 0.25\%$ for $T = 0.26,\ 0.24,\ 0.2$.

Eqs. 43, 47 were therefore employed to calculate $K(q,t)$ as described in the next sections.

F. Polydispersity effects for $K(q,t)$

At long times comparable with the total sampling time $\Delta t_{\max}$ (cf. Appendix A), $t \sim \Delta t_{\max}$ (more precisely, at $t \gg \tau_T$, beyond the temperature wave relaxation time $\tau_T = n_0 c_{vs}/\left(\kappa q^2\right)$, where $c_{vs} = c_v(t \to \infty)$ is the static heat capacity per particle) the correction ΔK_* vanishes, so $K(q,t) \simeq K_L(t)$, and the isothermic static limit of the longitudinal modulus, $K_{TLs} = K_{TL}(t \to \infty)$, can be approximated as

$$K_{TLs} \simeq K_L(t \sim \Delta t_{\max}) \simeq K_{TL}(t \sim \Delta t_{\max}) \tag{48}$$

On the other hand, the equilibrium static modulus $K_{\rm e}(q)$ can be obtained from the generalized compressibility equation[24,27,36]

$$S(q) = n_0 T / K_{\rm e}(q) \tag{49}$$

where

$$S(q) = \frac{1}{N}\left\langle \left| \sum_n e^{{\rm i}\underline{q}\cdot\underline{r}_n} \right|^2 \right\rangle \tag{50}$$

is the static structure factor. Using the $S(q)$ data for the 2D pLJ system we found that $K_{\rm e}(q)$ from eq. 49 ($= n_0 T/S(q)$) is significantly lower than the static modulus defined in eq. 48 even in the liquid regime, $\Delta t_{\max} \gg \tau_\alpha$, where τ_α is the structural α-relaxation time.

What is the reason for such a contradiction? In fact, it is related to the well-known matter that the standard compressibility equation[3] is violated in polydisperse systems, so

$$\lim_{q\to 0} S(q) \neq n_0 T / K_{TLs} \tag{51}$$

where the long-time limit of the isothermic longitudinal modulus $K_{TL}(t)$, $K_{TLs} \simeq \lim_{t\to\infty} K_{TL}(t)$, defines the isothermic compressibility κ_T in the liquid regime: $\kappa_T \simeq 1/K_{TLs}$. Physically this

discrepancy is due a coupling of composition fluctuations (which are absent in monodisperse systems) with fluctuations of the total concentration field $n(\underline{r})$ at any (however small) wave-vector $\underline{q}$. The mechanism of such coupling was elucidated in Ref. 36. To illustrate it let us consider a bidisperse mixture of small and large particles. A small longitudinal deformation ε of the system would lead to a concentration wave $\delta n(x) = n_0 \varepsilon e^{\mathrm{i}qx}$. Initially such deformation does not change the local composition of the system (the number fraction of small particles) which remains homogeneous, so $\delta n(x)$ implies a perturbation of the particle volume fraction $\delta\phi(x) \approx \varepsilon e^{\mathrm{i}qx}$ leading to a high free energy cost which is proportional to $\varepsilon^2 K_{TLs}$ with high static modulus K_{TLs} for a nearly incompressible system. However, an exchange of small and large particles leading to a higher fraction of small particles in denser regions (and higher fraction of large particles in less dense regions) can significantly reduce $\delta\phi$ leading to a lower energy cost. As a result, the emerging compositional wave gives rise to a significant decrease of $K(q,t)$ at long times from K_{TLs} to $K_e(q) = n_0 T/S(q)$, since $S(q)$ significantly increases with the polydispersity degree.[36]

An analogous process of compositional relaxation leads to the terminal relaxation stage of the dynamical structure factor $S(q,t)$ in polydisperse systems:[36] (see also note[59])

$$S(q,t) \simeq (S(q) - n_0 T/K_{TLs}) \exp\left(-q^2 t D_s\right), \;\; t \gg \tau_T, \tau_\alpha \tag{52}$$

where the α-relaxation time τ_α normally coincides with the terminal relaxation time for $G(t)$. The time-scale of this process is defined by the mean inter-diffusion coefficient D_{inter} of the particles, which nearly equals their self-diffusion coefficient D_s, $D_{inter} \approx D_s$, in weakly polydisperse systems.[36] The terminal relaxation time of $K(q,t)$ is related to D_s as well, but there is an important difference: while the terminal relaxation of $S(q,t)$, eq. 52, is mostly driven by the ideal-gas entropy of mixing of polydisperse particles, the $K(q,t)$ relaxation process is driven by the much higher elastic free energy of the longitudinal deformation which is proportional to K_{TLs}. More precisely, according to the FDT[36], the function $S(q,t)$ defines the concentration response $\delta n_q(t)$ to a weak external field $U(\underline{r},t) = U_q e^{\mathrm{i}\underline{q}\cdot\underline{r}}$ applied to the system at $t \geq 0$:

$$\delta n_q(t) = \frac{n_0}{T} U_q \left[S(q) - S(q,t)\right] \tag{53}$$

(ensemble-averaging as assumed in the l.h.s. of the above equation). Importantly, the definition of $K(q,t)$ implies that an analogous field (denoted as U_q^* in this case) is applied to the system to keep the longitudinal deformation (at wave-vector $\underline{q}$) constant (i.e., independent of time), so that the concentration perturbation $\delta n_q^*(t) = n^{\mathrm{def}}$ is constant as well. The difference between the

two cases is that U_q in eq. 53 is constant (at $t \geq 0$), while U_q^* is time-dependent. A meaningful comparison between the two cases demands that the terminal $\delta n_q(t \to \infty)$ in eq. 53 must be equal to n^{def} (to ensure that all particle components are eventually distributed in the same way in both cases). Therefore we get

$$U_q = \frac{n^{\mathrm{def}} T}{n_0 S(q)} \tag{54}$$

Let us consider the very beginning of the particle interdiffusion process ($\tau_T, \tau_\alpha \ll t \ll 1/(q^2 D_s)$). The interdiffusion rate is then driven by the external field U_q (in the case of eq. 53) and by U_q^* in the case of longitudinal relaxation modulus, hence

$$D^*/D_s = U_q^*/U_q \tag{55}$$

where D^* is the effective interdiffusion constant relevant for $K(q,t)$. The amplitude U_q^* can be found by minimization of the effective free energy

$$\frac{1}{2} K_{TLs} \left(\delta n_q^*/n_0\right)^2 - U_q^* \delta n_q^*$$

leading to

$$U_q^* = K_{TLs} n^{\mathrm{def}}/n_0^2 \tag{56}$$

Using eqs. 54, 55, 56 we get the effective diffusion constant for the terminal relaxation of the longitudinal modulus:

$$D^* = D_s K_{TLs}/K_{\mathrm{e}}(q) \tag{57}$$

The terminal compositional relaxation stage of $K(q,t)$ is therefore given by the following equation (an alternative derivation of eq. 58 is presented in section IV):

$$K(q,t) \simeq K_{TLs} + (K_{\mathrm{e}}(q) - K_{TLs}) \left[1 - \exp\left(-q^2 t D_s K_{TLs}/K_{\mathrm{e}}(q)\right)\right], \; t \gg \tau_T, \tau_\alpha \tag{58}$$

This equation assumes that the self-diffusion is Fickian. In the general case (in particular, at $T \lesssim T_g$) it is the mean-square particle displacement (MSD) that matters, so tD_s must be replaced with

$$h_0(t) = \frac{1}{2d} \left\langle \left| \underline{r}_a(t+t') - \underline{r}_a(t') \right|^2 \right\rangle \tag{59}$$

where averaging over all particles (index a) is assumed in the rhs Combining thus modified eq. 58 with eqs. 47, 43 we get the final approximate result:

$$K(q,t) \approx K_L(t) + \frac{T}{n_0} \frac{p_{T0}(t)^2}{c_{v0}(t)} \exp\left(-\frac{\kappa q^2 t}{n_0 c_{v0}(t)}\right) +$$

$$+(K_{\rm e}(q)-K_{TLs})\left[1-\exp\left(-q^2h_0(t)K_{TLs}/K_{\rm e}(q)\right)\right] \tag{60}$$

This equation is used in the next section to predict different q,t-resolved correlation functions. The functions entering the rhs of eq. 60 have been considered above: The longitudinal modulus $K_L(t)$ is defined in eq. 8, the bulk shear modulus $G(t)$ is obtained based on the stress-fluctuation relation;[10] the bulk compression modulus $K_0(t)$, the thermal pressure $p_{T0}(t)$ and the heat capacity $c_{v0}(t)$ are obtain based on pressure and energy auto- and cross-correlation functions as described in ref. 10. $h_0(t)$ comes from the particle MSD; $K_e(q)$ is defined by the standard structure factor $S(q)$ using eq. 49. Finally the heat conductivity κ is obtained as described in Appendix B. The eventual time-dependence of $K(q,t)$ at $T=0.4$ and 0.3 is illustrated in Fig. 2.

III. THEORY FOR q,t-RESOLVED TENSORIAL STRESS CORRELATION FUNCTIONS

A. The dynamical structure factor

Before turning to stress correlations we chose to verify the basic result of the previous section, eq. 60. To this end let us consider the dynamical structure factor

$$S(\underline{q},t)=\frac{1}{N}\sum_{a,a'}\left\langle\exp\left(\mathrm{i}\underline{q}\cdot\left(\underline{r}_a(t+t')-\underline{r}_{a'}(t')\right)\right)\right\rangle \tag{61}$$

where a,a' run over all particles in the system, and an averaging over t' is assumed. For macroscopically isotropic systems only the magnitude of $\underline{q}$ is relevant,[55] so $S(\underline{q},t)$ can be averaged over orientations of $\underline{q}$. The linear response theory leads to the following rigorous relation[24,27] between $K(q,t)$ and $S(q,t)$:

$$S(q)-S(q,s)=T\left[ms^2/q^2+K(q,s)/n_0\right]^{-1} \tag{62}$$

where $S(q,s)$ is the modified Laplace transform (defined in eq. 26) of $S(q,t)$. The above equation shows that $\frac{\partial S(q,t)}{\partial t}=0$ and $\frac{\partial^2 S(q,t)}{\partial t^2}=-\frac{T}{m}q^2$ at $t=0$.

The relation, eq. 62, comes from the FDT (or the Zwanzig-Mori projection operator formalism)[3,4,37]; it is general and exact provided that all particles have the same mass. It allows to predict $S(q,t)$ based on the known $K(q,t)$. The latter was calculated using eq. 60 and the classical time-dependent correlation functions for $q=0$ involved in it (like $K_L(t)$, $c_{v0}(t)$, $h_0(t)$) obtained using simulation data for the 2D pLJ system (Appendix A). A multi-exponential approximation was then

applied to the function $K(q,t)$ at a given q (cf. point 6 of section IV for further discussion):

$$K(q,t) = \sum_i K_i e^{-\gamma_i t} \tag{63}$$

Here $i = 0, 1, \ldots, i_m$, with non-negative γ_i and real K_i, $\gamma_0 = 0$ and $K_0 > 0$. $K_0 = K_e(q) \equiv n_0 T/S(q)$ in the liquid regime ($T > T_g$) when a full relaxation of the system can be achieved. (The number of modes in eq. 63 and in the analogous eq. 76 was around 25.) At low temperatures, $T \lesssim T_g$, K_0 should be treated as a quasi-static longitudinal modulus at $t \sim \Delta t_{\max}$, $K_0 = K_{TLs}$ (here $\Delta t_{\max}$ is the total sampling time, see Appendix A). The s-transform of K therefore is

$$K(q,s) = \sum_i K_i \frac{s}{s+\gamma_i} \tag{64}$$

The general expressions for $S(q,t)$ and $S(q,s)$ can be then deduced from eqs. 62, 64:

$$S(q,s) = Y_0 + \sum_k Y_k \frac{s}{s-r_k}, \;\; S(q,t) = Y_0 + \sum_k Y_k \exp(r_k t) \tag{65}$$

where $k = 1, 2, \ldots, i_m + 2$, r_k are the roots of the equation $smn_0/q^2 + K(q,s)/s = 0$ (hence, r_k are roots of a polynomial of order $i_m + 2$) and Y_0, Y_k are constants. Furthermore, using again eq. 62 and eq. 65 we get:

$$S(q,s) = Y_0 + \sum_k Y_k + \sum_k \frac{Y_k r_k}{s-r_k}, \;\; Y_0 = S(q) - \sum_k Y_k \tag{66}$$

where

$$Y_k = \frac{n_0 T}{r_k^2} \left[\sum_i \frac{K_i}{(r_k+\gamma_i)^2} - \frac{mn_0}{q^2} \right]^{-1} \tag{67}$$

Hence, finally the dynamical structure factor becomes

$$S(q,t) = S(q) + \sum_k Y_k \left[\exp(r_k t) - 1 \right] \tag{68}$$

The theoretical predictions based on eq. 68 are compared in Fig. 3 with the simulation data for $S(q,t)$ obtained directly using its definition, eq. 61 (the amplitudes K_i involved in eq. 67 have been obtained by minimization of the mean-square deviation between the prescribed $K(q,t)$ and its multi-exponential approximation, eq. 63). A good agreement between the theory and simulation data for $S(q,t)$ is obvious, which means that the basic approximation, eq. 60, works well both above and below T_g.[44]

B. Stress correlation functions

The time-space resolved stress correlation tensor is defined as

$$C_{\alpha\beta\alpha'\beta'}(\underline{q},t) = \frac{V}{T}\left\langle \delta\sigma_{\alpha\beta}\left(\underline{q},t+t'\right)\right) \delta\sigma_{\alpha'\beta'}\left(-\underline{q},t'\right)\right)\rangle \tag{69}$$

where $\delta\sigma_{\alpha\beta}\left(\underline{q},t\right) = \sigma_{\alpha\beta}\left(\underline{q},t\right) - \left\langle \sigma_{\alpha\beta}\left(\underline{q},t'\right)\right\rangle$ (note that $\left\langle \sigma_{\alpha\beta}\right\rangle = 0$ for $q \neq 0$). In two dimensions the full correlation tensor $C_{\alpha\beta\alpha'\beta'}$ of a macroscopically isotropic system is completely defined by four independent components[6]: $C_{1212} \equiv C_s$, $C_{1111} \equiv C_{\|}$, $C_{1122} \equiv C_{\perp}$, and $C_{2222} \equiv C_2$, where axis '1' is chosen to be parallel to $\underline{q}$, while axis '2' is perpendicular to it (cf. eq. 103). As shown elsewhere[3,4,24,37,38] the first two correlation functions (C_s and $C_{\|}$) are directly related to the generalized moduli considered above:

$$C_s(q,s) = \frac{\rho s^2 G(q,s)}{\rho s^2 + q^2 G(q,s)} \tag{70}$$

$$C_{\|}(q,s) = \frac{\rho s^2 K(q,s)}{\rho s^2 + q^2 K(q,s)} \tag{71}$$

where (as before) $\rho = mn_0$ is the mean mass density, s is the Laplace parameter conjugate to time, and the functions $C_s(q,s)$, etc. are the s-transforms defined in eq. 26. These equations come from the FDT (the linear response theory) or from the Zwanzig-Mori projection operator formalism; they are exact as such in the thermodynamic limit. An analogous equation for $C_{\perp}(q,s)$ comes from the FDT as well[6]:

$$C_{\perp}(q,s) = \frac{\rho s^2 M(q,s)}{\rho s^2 + q^2 K(q,s)} \tag{72}$$

Here $M(q,s)$ is the s-transform of the transverse modulus $M(q,t)$ defined by the normal stress response in the direction perpendicular to the elongation axis

$$M(q,t) = \lim_{\varepsilon_{11}\to 0} \frac{\Delta\sigma_{22}(\underline{q},t)}{\varepsilon_{11}} \tag{73}$$

where ε_{11} is the elongation strain applied at $t = 0$. At $q = 0$ this modulus is directly related to the shear and longitudinal moduli:

$$M(0,t) = K(0,t) - 2G(0,t) = K_L(t) - 2G(t)$$

due to the global isotropy of the system. This relation stays approximately valid also at low $q \neq 0$ since a shear response is local (cf. section II C), while the relevant non-local (conserved) fields

(like energy density and composition) that affect the normal pressure are scalar and hence provide equal contributions to $M(q,t)$ and $K(q,t)$, so

$$M(q,t) \simeq K(q,t) - 2G(q,t), \;\; 2\pi/q \gg \bar{b} \tag{74}$$

This approximation is used in the next section.

The 4th relation involving C_2 was derived in Refs. 6, 20, and 21 for monodisperse isothermic systems (i.e., for the limit $\kappa \to \infty$). Following the argument of Ref. 6 (based on the concept of structural stress noise) we show that in the general case (including polydisperse systems) the relation between C_2 and relaxation moduli reads

$$C_2(q,s) \simeq K(q,s) - \frac{q^2 M(q,s)^2}{\rho s^2 + q^2 K(q,s)} \tag{75}$$

At this point it is worth stressing again that in the general case (when the longitudinal stress relaxation is coupled with 'conserved' scalar fields like energy and composition), it is important to take into account the q-dependence of the moduli. Eq. 75 is approximate: it is valid asymptotically at low q's (i.e., in the hydrodynamic regime $\lambda = 2\pi/q \gg \bar{b}$).

The above four relations for the stress correlation functions are verified below based on our simulation data for the 2D pLJ system.

C. Comparison with simulation data

The stress correlation functions can be predicted using the relations of the previous section involving two generalized relaxation moduli, $G(q,t)$ and $K(q,t)$. These relaxation functions are approximately defined in eqs. 19, 60. The function $C_{\parallel}(q,t)$ can be obtained based on the known $K(q,t)$ in exactly the same way as the dynamical structure factor, cf. section III A. $C_s(q,t)$ was obtained analogously starting with the multi-exponential approximation of $G(q,t)$, cf. eq. 63:

$$G(q,t) \simeq G(t) = \sum_i G_i e^{-\gamma_i t} \tag{76}$$

with real G_i and positive γ_i, leading eventually to a similar representation of $C_s(q,t)$, but generally with complex amplitudes and rates, cf. eq. 68. We checked that different approximations of $G(t)$ (different choices of the relaxation rate set $\{\gamma_i\}$) lead to virtually identical results for $C_s(q,t)$.

The remaining two relations, eqs. 72, 75, can be used to obtain $C_{\perp}(q,t)$ and $C_2(q,t)$ in a similar fashion. The theoretical predictions for all the four stress correlation functions are compared

with our simulation data at different temperatures T and wave-vectors q. The results are shown in Figs. 4, 5, 6, 7. At $T = 0.4, 0.3$ (above the glass transition) there is a complete agreement for all correlation data (the black theoretical curve is virtually invisible at $t > 6$ being completely overlapped by the red data curve, see Fig. 4(a),(b)). The shear stress correlations C_s show a few decaying oscillations reflecting transient shear acoustic waves. As for the correlations of normal stresses ($C_\parallel$, $C_\perp$, C_2), they show much more pronounced oscillations which decay more slowly. These oscillations correspond to longitudinal sound waves. Their decay time ($\sim 100 \div 200$) increases as the temperature is lowered. Turning to the autocorrelation function C_2, we note a remarkable feature emerged at $T = 0.3$: the oscillations are now significantly asymmetric pointing to a monotonic slowly decaying process. This slow process is even more apparent at $T = T_g = 0.26$, where it persists beyond the oscillation relaxation time. The relaxation time of the slow process at $T = 0.26$ is $\tau_{slow} \sim 10^4$. By contrast, the total sampling time $\Delta t_{\max} = 10^5$ is not enough for its relaxation at $T = 0.24$. Furthermore, at $T = 0.2$ (well below the glass transition) any relaxation of $C_2(q,t)$ is hardly visible for $t \gtrsim 500$ (cf. Fig. 4(e)). As for all other correlation functions ($C_\parallel$, $C_\perp$, C_s), they always relax during a time $\tau_{atn} \lesssim 500$ which is nearly the same for all the 3 functions at $T \leq T_g$. Apparently τ_{atn} is the attenuation time for the relevant sound waves (both shear and longitudinal, cf. points 4 and 8 of section IV for further discussion), while τ_{slow} is proportional to the structural α-relaxation time τ_α. Overall, for $q = q_{min} \equiv 2\pi/L$ we observe an excellent agreement between the theory and simulation data for all the stress correlation functions, all temperatures and in the whole sampling time range. A close inspection of the graphs at low T's reveals some disagreement in a time range around $t \sim 200$. This feature may seem surprising given the agreement at both shorter and longer times t. However, there is a simple reason for it: the stress correlation functions based on the simulation data were smoothed at $t \gtrsim 100$ to accelerate their calculation, and this procedure led to a reduction of the oscillation amplitude as can be observed in Figs. 4 (d),(e) (see red curves there).

The effect of the wave-vector q is demonstrated in Figs. 5, 6, 7. Generally, the oscillation regime becomes shorter and with higher frequency, as expected, for larger q. Beyond this regime the stress correlations vanish except for autocorrelations of the second normal stress, C_2. At $T = 0.3$ the positive monotonic long-time tail of C_2 becomes more pronounced at higher q (see Fig. 5 (b),(c)). It appears that the theory slightly underestimates the terminal relaxation time of C_2 at the highest q's (see Fig. 5(c)). Otherwise the agreement between the theory and simulations stays quite good up to $q \sim 8q_{\min}$ corresponding to $q\bar{b} \sim 0.5$. Below the glass transition, at $T = 0.24$, the

agreement is nearly as good for C_s, $C_\parallel$, $C_\perp$ (see Fig. 6). However, to get a similar agreement for the autocorrelation function of transverse stress, C_2, for the highest q's we had to vertically shift the theoretical curve by a constant Δ: $C_2 \to C_2 + \Delta$, with $\Delta = 1.9$ for $n_{q2} \equiv \left(q/q_{\min}\right)^2 = 32$, and $\Delta = 2$ for $n_{q2} = 64$. Such a shift was also applied at $T = 0.20$ (see Fig. 7): $\Delta = 4.7$ for $n_{q2} = 8$, $\Delta = 1.2$ for $n_{q2} = 32$ and $\Delta = 1.13$ for $n_{q2} = 64$. The origin of this shift is discussed in point 12 of section IV. Moreover, Fig. 6 indicates that the terminal relaxation time of the simulated C_2 slightly increases at the highest q's ($n_{q2} = 32,\ 64$) at $T = 0.24$ (see Fig. 6). To sum up, it would be fair to say that the agreement between the theory and simulations is very good for the functions C_s, $C_\parallel$ at all temperatures and wave-vectors with $n_{q2} \leq 64$ (which corresponds to $q\bar{b} \lesssim 0.5$). A small discrepancy (with relative error typically within 5%) can be observed for $C_2(q,t)$ in the terminal relaxation regime for the highest q's at low T.

IV. DISCUSSION

1. As we pointed out in section II C, while the bulk longitudinal modulus $K_L(t)$ depends on the thermostatting method, the generalized longitudinal modulus $K(q,t)$ is universal, that is independent of a coupling of the system with a thermostat. Such universality also holds for the bulk adiabatic and isothermic moduli, $K_{AL}(t)$ and $K_{TL}(t)$, which can be obtained using the theoretical approach proposed in Ref. 10. For low q the generalized modulus $K(q,t)$ of a monodisperse system can be expressed in terms of $K_{AL}(t)$ or $K_{TL}(t)$ and other bulk response functions, cf. eqs. 37, 39.

Noteworthily, the isothermic *longitudinal* modulus $K_{TL}(t)$ can be defined via the normal pressure (p_{xx}) response to a small compression in the x-direction, $\varepsilon = -\varepsilon_{xx}$ (more precisely, a canonic affine transformation of coordinates and velocities of all particles defined in eq. 6) at *constant transverse area* (of the cross-section perpendicular to the deformation axis) and constant temperature: $\Delta p_{xx}(t) = K_{TL}(t)\varepsilon$. The adiabatic longitudinal modulus $K_{AL}(t)$ is defined in a similar way: $K_{AL}(t) = \lim_{\varepsilon\to 0} \Delta p_{xx}(t)/\varepsilon$, where it is the total energy E that is kept constant after the canonic-affine uniaxial compression at $t = 0$. In a similar fashion, $c_{pL}(t)$ (cf. Appendix B) is the heat capacity at constant *longitudinal* normal pressure p_{xx} and constant transverse area (no deformation in the plane perpendicular to the x-axis). $c_{pL}(t)$ is different from the standard isobaric heat capacity $c_p(t)$; it is related to $c_v(t)$:

$$c_{pL}(s) = c_v(s) / \left[1 - \frac{T}{n_0} \frac{p_T(s)^2}{c_v(s) K_{AL}(s)}\right] = c_v(s) \frac{K_{AL}(s)}{K_{TL}(s)} \tag{77}$$

The above equation involve s-transforms of the time-dependent functions; it was obtained in analogy with the argument considered in section II D. Therefore $c_{pL}(s)/c_v(s) = K_{AL}(s)/K_{TL}(s)$; this equation is analogous to the more standard relation $c_p(s)/c_v(s) = K_A(s)/K_T(s)$ (cf. eqs. (D23), (D25) in Ref. 10).

2. The generalized longitudinal modulus $K(q,t)$ for monodisperse systems is defined in eqs. 37, 39. It is remarkable that these equations can be obtained rather easily by first *assuming* that all response functions (K_{AL}, p_T, c_v) are constants and therefore can be expressed via the thermodynamic derivatives. Then, in the final relation each constant must be replaced by a function of the Laplace parameter s, i.e., by the modified Laplace transform (cf. eq. 26) of the corresponding response function. We emphasize that this trick, which was already hinted at[10,38], works precisely with the modified Laplace transforms, and generally not in the time domain.

3. It is noteworthy that the heat conductivity κ (involved in eqs. 37, 39) was obtained by fitting the simulation data for the autocorrelation function of temperature, $C_T(q,t)$, with the theoretical equation coming from the generalized hydrodynamics (see Appendix B). It turns out that κ is nearly constant (independent of q) at low q, $\lambda = 2\pi/q \gg \bar{b}$. We found however that κ somewhat decreases with q for $q\bar{b} \gtrsim 0.5$. The frequency dependence of the conductivity κ (or it dependence on the Laplace parameter s) can be totally neglected for low q ($\lambda \gg \bar{b}$) since the microscopic time $\sim \tau_v$ relevant for the heat conduction (here τ_v is the time of particle velocity relaxation by collisions and vibrations) is much shorter than the characteristic time of thermal diffusion process, $\tau_T = 1/\left(D_T q^2\right)$, cf. eq. 78.

4. The generalized longitudinal modulus $K(q,t)$ shows a shoulder at $t \sim \tau_T \lesssim 10 \div 100$ corresponding to the transition from adiabatic to isothermic response due to heat conduction (cf. Figs. 1, 2). The characteristic time of this process, $\tau_T = 1/\left(D_T q^2\right)$, is defined by the isochoric thermal diffusivity

$$D_T = \frac{\kappa}{n_0 c_{vs}} \tag{78}$$

which is relevant here since $K(q,t)$ is a response to a small strain (ε) kept constant at $t > 0$ is the equilibrium specific heat). All the three parameters involved in the above equation (thermal conductivity κ, particle concentration n_0 and the heat capacity per particle, c_v)[45] just weakly depend on temperature T for the 2D pLJ system we studied. Therefore, the thermal diffusion time τ_T is almost independent of T: $\tau_T \sim 50$ for $q = q_{\min}$ (cf. Fig. 1). Well above $T_g \approx 0.26$ the time τ_T for $q = q_{\min}$ is longer than the structural relaxation τ_α as defined by the shear relaxation modulus

$G(t)$, however, τ_α exceeds τ_T at $T \lesssim 0.3$ (cf. Fig. 10 in Ref. 10).

Remarkably, the attenuation time τ_L of oscillations in the dynamical structure factor $S(q,t)$ and the stress-correlation functions ($C_\parallel(q,t)$, $C_\perp(q,t)$, $C_2(q,t)$) shows a similar q-dependence as τ_T (see eq. 84). However, the attenuation time τ_L is longer than τ_T and the ratio $\tau_L/\tau_T \sim 2 \div 5$ increases at low T (cf. Figs. 3, 4). A comparison of eqs. 84 and 78 shows that this effect is due to a decrease of the nondimensional ratio $\eta_L/(\kappa m)$ on cooling below T_g, where η_L is the relevant (for attenuation) longitudinal viscosity (cf. the text around eq. 84).

5. The terminal stage of relaxation for the dynamical structure factor $S(q,t)$ of a polydisperse system is defined in eq. 52; it is related to composition fluctuations (cf. Ref. 36). Eq. 52 is based on the assumption that the free energy cost of a relevant ('soft') composition fluctuation mainly comes from the ideal-gas entropy, hence the relevant interdiffusion constant is close to the self-diffusivity D_s of the particles. This assumption is generally valid for systems with sufficiently weak polydispersity. It was verified for the 2D pLJ system we studied.[36]

Furthermore, the terminal relaxation of the longitudinal modulus $K(q,t)$, eq. 58, can be derived from eq. 52 based on the general eq. 62: For $t \gg \tau_L$ the term ms^2/q^2 in the rhs of eq. 62 can be neglected (since the attenuation time of oscillations in $K(q,t)$ is much longer than the oscillation period), hence we get

$$K(q,s) \simeq \frac{n_0 T}{S(q)-S(q,s)}, \;\; S(q,s) \simeq (S(q)-n_0T/K_{TLs})\frac{s}{s+q^2D_s}$$

The above equations lead to eq. 58 upon doing the inverse s-Laplace transform.

Finally, the validity of eq. 52 at $t \gtrsim 100$, and the relevance of composition fluctuations is demonstrated in Fig. 10, where we plot the dynamical structure factor, $S(q,t)$, based on our simulation data, its long-time approximation of eq. 52 and the dynamical composition structure factor, $S_\psi(q,t)$, again directly obtained by simulations. Here $S_\psi(q,t)$ is defined analogously to eq. 61 but with the prefactor $\kappa_a\kappa_{a'}$ before the exponential, where $\kappa_a = b_a^2/\overline{b^2} - 1$ is positive for large and negative for small particles. The function $S_\psi(q,t)$ is thus related to the correlation function of the composition order parameter $\psi(\underline{r},t) = \sum_a \kappa_a \delta(\underline{r}-\underline{r}_a)$ which equals to zero on the average. Fig. 10 clearly shows that the long-time relaxation of $S(q,t)$ is an interdiffusion process following the decay of composition fluctuations quantified by $S_\psi(q,t)$.

6. To facilitate direct and inverse Laplace transformations of the stress-correlation functions (cf. eqs. 70, 71) involving the generalized moduli, $G(q,t)$, $K(q,t)$, we employed multi-exponential approximations of their time-dependencies (see eqs. 76, 63). This approach formally corresponds

to the generalized Maxwell model[31] for the shear relaxation modulus $G(t)$. Noteworthily, the Maxwell model implicitly assumes that inertial effects are negligible for the structural dynamics. In this case the generalized Brownian dynamics (involving stochastic moves in the configurational space) are applicable, and the detailed balance dictates that all amplitudes in eq. 76 must be positive, so the relaxation function $G(q,t)$ must monotonically decrease in time. Such relaxation behavior is exhibited, in particular, with the MC dynamics. A similar behavior is expected for $K(q,t)$. The molecular dynamics (MD) employed in the present study does account for inertial effects (which are normally important at short t), hence negative amplitudes (G_i or K_i) must be allowed as well. Note that in this general case the relaxation moduli can still be uniformly approximated with multi-exponentials to an arbitrarily high precision as follows from the Weierstrass-Bernstein approximation theorem.

7. Using eqs. 70, 71, 72, 74, 75 one can easily get the stress correlations at $t = 0$ (at no time-shift):

$$C_s(q,0) = G_A(q), \;\; C_{\|}(q,0) = K_{AL}(q) \tag{79}$$

$$C_{\perp}(q,0) \simeq K_{AL}(q) - 2G_A(q), \;\; C_2(q,0) \simeq K_{AL}(q) \tag{80}$$

where $G_A(q) = G(q,0)$ and $K_{AL}(q) = K(q,0)$ are q-dependent generalizations of affine (bulk) shear modulus μ_A and longitudinal modulus $\eta_{AL} \equiv \eta_A + (2-2/d)\mu_A$, and $\mu_A = G(0)$, $\eta_{AL} = K_{AL}(0)$.[46] The moduli $G_A(q)$ and $K_{AL}(q)$ define the immediate stress response to the generalized shear ($\gamma > 0$, $\varepsilon = 0$) and longitudinal ($\gamma = 0$, $\varepsilon < 0$) deformations, eqs. 12, 13. These deformations are not affine for $q \neq 0$, but they are always adiabatic. Note that eqs. 79 are exact, while eqs. 80 are expected to be approximately valid for $2\pi/q \gg \bar{b}$. Their precision can be assessed using simulation data for the stress correlation functions at $t = 0$. Note that the adiabatic moduli $K_{AL}(q) = K(q,0)$ and $K_{AL}(t) = K(q \to 0, t)$ are different functions, but $K_{AL}(q \to 0) = K_{AL}(t \to 0)$.

8. Turning to the stress correlation function at $t > 0$, we observe that initial shear (σ_{21}) and longitudinal (σ_{11}) stresses generate body forces $\underline{f}$ on the system elements:

$$f_2 = \mathrm{i}q\sigma_{12}e^{\mathrm{i}qx}, \; f_1 = \mathrm{i}q\sigma_{11}e^{\mathrm{i}qx} \tag{81}$$

(here we assume for simplicity that the wave-vector $\underline{q}$ and therefore axis 1 are parallel to the x-axis). These forces in turn generate shear and longitudinal sound waves. Their frequencies ω_s, ω_L are defined by the relevant shear, c_s, and longitudinal, c_L, sound velocities:

$$\omega_s = qc_s, \;\; \omega_L = qc_L; \;\; c_s \simeq \sqrt{G'(q,\omega_s)/\rho}, \;\; c_L \simeq \sqrt{K'(q,\omega_L)/\rho} \tag{82}$$

where $G'(q,\omega)$ is the storage shear modulus equal to the real part of $G(q, s = \mathrm{i}\omega)$:

$$G(q, s = \mathrm{i}\omega) = G'(q,\omega) + \mathrm{i}G''(q,\omega) \tag{83}$$

The longitudinal storage modulus $K'(q,\omega)$ is related to $K(q,s)$ (the s-transform of $K(q,t)$) in a similar way. The shear oscillations with frequency ω_s are reflected in the time-dependence of $C_s(q,t)$, while the longitudinal frequency ω_L is relevant for $C_{\|}(q,t)$, but also for the dynamical structure factor $S(q,t)$ (cf. Fig. 3) and auto- and cross-correlations of normal stresses, $C_2(q,t)$, $C_{\perp}(q,t)$ (cf. Fig. 4). With the data for the pLJ system at hand (cf. Ref. 10 and Fig. 1) we estimate $c_s \sim 2 \div 4$, $c_L \sim 8 \div 9$ using eqs. 82 in the most interesting temperature regime $T = 0.3 \div 0.2$ (around the glass transition at $T_g \approx 0.26$). These estimates correspond to the oscillation periods for $q = q_{\min}$, $\frac{2\pi}{\omega_s} \sim 40 \div 25$, $\frac{2\pi}{\omega_L} \sim 12$, in agreement with the data shown in Fig. 4. The attenuation times of these oscillations (τ_s for $C_s(q,t)$, and τ_L for other functions) are defined by effective viscosities η_s, η_L:

$$1/\tau_s \simeq \frac{\eta_s}{2\rho} q^2, \;\; 1/\tau_L \simeq \frac{\eta_L}{2\rho} q^2 \tag{84}$$

where the relevant viscosities are related to the dynamical loss moduli, $G''(q,\omega)$ and $K''(q,\omega)$[50]

$$\eta_s = G''(q,\omega_s)/\omega_s, \;\; \eta_L = K''(q,\omega_L)/\omega_L \tag{85}$$

Note that the viscosities defined in the above equation are dynamical in nature; they are generally different from the classical viscosities obtained in the low-frequency limit. The correlation functions presented in Fig. 4 show comparable sound attenuation times, $\tau_s \sim \tau_L$, in the regime $0.2 \leq T \leq 0.3$; the times increase from $\tau_L \sim 100$ to $\tau_L \sim 300$ on cooling. This means that the relevant effective viscosities are also comparable and *decrease* as the system is cooled below the glass transition. The dynamic viscosities η_s, η_L therefore show an opposite temperature dependence as compared to the steady shear viscosity which is proportional to the α-relaxation time.

Interestingly, the low-frequency ($s \to 0$) limit of the longitudinal compression modulus $K(q,s)$, obtained using eqs. 43, 44, is:

$$K^{\text{hydro-limit}}(q,s) \simeq K_{TLs} + s\left[\zeta + 2\left(1 - \frac{1}{d}\right)\eta + \frac{K_{TLs}(\gamma - 1)}{s + D_T q^2}\right], \tag{86}$$

where K_{TLs} ($= \eta_{\mathrm{A}} - TC_p(0)/n_0$) is the isothermal compression modulus, $\gamma = c_{ps}/c_{vs}$ with c_{ps} and c_{vs} being respectively the equilibrium specific heat at constant pressure and at constant volume, $D_T = \kappa/(n_0 c_{vs})$, the thermal diffusivity, and ζ and η the bulk and shear viscosity, respectively.

The viscosities are defined by

$$\zeta = \frac{T}{n_0}\int_0^\infty C_p(t)\mathrm{d}t, \;\; \eta = \int_0^\infty G(t)\mathrm{d}t \tag{87}$$

Noteworthily, on the one hand Eq. 86 is consistent with the results obtained for $d = 3$ and $\kappa \to \infty$ in Ref. 27 (see text below eq. (12) there). On the other hand, for finite κ the term in square brackets of Eq. 86 agrees with Eq. (3.104b) in Götze's book[37].

9. It is obvious from Figs. 4 - 7 that all stress correlation functions except $C_2(q,t)$ rapidly vanish beyond the attenuation time τ_s or τ_L. By contrast, $C_2(q,t)$ shows a long-time monotonically decaying tail. What is the origin of this difference? Firstly, we observe that the 3 correlation functions, C_s, $C_\parallel$, $C_\perp$ involve shear or longitudinal stresses, $\sigma_{12} = \sigma_{21}$ and σ_{11}, which generate a body force (cf. eq. 81). Therefore their long-time presence (for $t \gg \tau_s,\ \tau_L$) would contradict mechanical equilibrium of the system, hence these stresses must rapidly vanish also in the glassy regime, $T < T_g$. As for the function $C_2(q,t)$, it involves only the transverse normal stress σ_{22} which does not generate any fluid motion (the body force associated with this component of stress field is identically zero since $\underline{q}$ is normal to axis 2), so $\sigma_{22}(q,t)$ may stay unchanged for a long time. Generally, the long-time tail of $\sigma_{22}(q,t)$ is defined by the structural processes reflected also in the relaxation moduli $G(q,t) \simeq G(t)$ and $K(q,t)$; it may persist virtually forever in amorphous systems at low T. We therefore arrive at the concept of a quenched (or frozen) stress, which is equal to the mean stress $\bar{\sigma}_{\alpha\beta}(\underline{q})$ (=time-average of $\sigma_{\alpha\beta}(\underline{q},t)$): The stress tensor in a glassy state (i.e., a metabasin of the free energy landscape) can be therefore written as

$$\delta\sigma_{\alpha\beta}(\underline{q},t) = \tilde{\sigma}_{\alpha\beta}(\underline{q},t) + \bar{\sigma}_{\alpha\beta}(\underline{q}) \tag{88}$$

where $\tilde{\sigma}_{\alpha\beta}(\underline{q},t)$ is the fluctuation part whose time-average is zero. Eq. 88 obviously implies that

$$\lim_{t\to\infty} C_{\alpha\beta\alpha'\beta'}(\underline{q},t) = \frac{V}{T}\left\langle \bar{\sigma}_{\alpha\beta}(\underline{q})\bar{\sigma}_{\alpha'\beta'}(-\underline{q})\right\rangle \tag{89}$$

From the above discussion it is clear that the only non-zero component of $\bar{\sigma}_{\alpha\beta}(\underline{q})$ is $\bar{\sigma}_{22}(\underline{q})$ (recall that we consider 2D systems in the present paper). Therefore, C_2 tends to a finite limit at long time,

$$C_2(q,t) \to \left\langle \frac{V}{T}\left|\bar{\sigma}_{22}(\underline{q})\right|^2 \right\rangle \equiv \theta(q), \;\; t\to\infty \tag{90}$$

in the amorphous solid regime well below T_g (where the relaxation time τ_α can be considered as infinite). The $\langle ...\rangle$ brackets here imply also averaging over different orientations of $\underline{q}$. Such behaviour can be indeed observed in Figs. 4 - 7.

10. As discussed above the stress correlation functions $C_{\|}(q,t), C_{\perp}(q,t), C_s(q,t)$ rapidly vanish for $t \gtrsim \tau_L$. The behavior of the transverse normal stress autocorrelation function $C_2(q,t)$ is different at $T \lesssim T_g$: it shows a slow monotonic decay at $t \gtrsim 2\tau_L$ (the time τ_L is defined in eq. 84). This monotonic regime can be analyzed using eq. 75 leading to the following approximate result:

$$C_2(q,t) \approx 4G(t)\left[1 - \frac{G(t)}{K(q,t)}\right], \;\; t \gtrsim 2\tau_L \tag{91}$$

We verified that the above equation does a fair job at $t \gtrsim 2\tau_L$ and $q\bar{b} \lesssim 0.5$ and agrees with the results of the full numerical analysis based on eq. 75 (cf. section III C) within an accuracy of $\sim 1\%$. Moreover, we found that $K(q,t)$ in eq. 91 can be replaced with just $K_{TL}(t)$ since the terminal decay of $K(q,t)$ (by the interdiffusion process) occurs at times longer than the relaxation time τ_α of $G(t)$ for the studied range of wavevector q. Hence (with accuracy of $\sim 5\%$)

$$C_2(q,t) \approx 4G(t)\left[1 - \frac{G(t)}{K_{TL}(t)}\right], \;\; t \gtrsim 2\tau_L \tag{92}$$

This equation shows that the relaxation time of $C_2(q,t)$ is comparable with τ_α.

11. The FDT relations, eqs. 70, 71, 72, and the relation 75, are based on the linear response theory, and are valid for equilibrium systems. The latter condition is not a problem in the liquid state, but amorphous systems (supercooled liquids below T_g) are normally out of the thermodynamic equilibrium. Are the quoted equations useful in this case? The answer is yes. The reason is that while amorphous systems are distributed over the glassy states in a non-equilibrium (and often unknown) way, they can still be well-equilibrated within each metabasin (glassy state).[9] In this case the dynamical (FDT-like) relations stay valid provided that a (generally unknown) time-independent constant is added in the rhs[5,9] (this constant term accounts for an unknown relation between the partition function in a glassy state and in its deformed counterpart). Eq. 89 ensures that the correlation functions C_s, $C_{\|}$, $C_{\perp}$ must tend to 0 at long times, so the additional constant must vanish for the corresponding FDT eqs. 70, 71, 72, which therefore stay unchanged also below T_g (note that the $t \to \infty$ limit of the theoretical rhs in any of these equations corresponds to $s \to 0$, so the rhs must tend to 0 in this limit). It is only eq. 75 that should be amended as

$$C_2(q,s) \simeq K(q,s) - \frac{q^2 M(q,s)^2}{\rho s^2 + q^2 K(q,s)} + \Delta(q) \tag{93}$$

to be generally valid also in the glassy regime.

Remarkably, the need for the Δ-correction for C_2 below T_g was demonstrated by the data shown in Figs. 6, 7 (with a vertical shift of the theoretical C_2 in some cases). It is tempting therefore

to attribute this correction simply to a non-equilibrium character of our systems below T_g. We, however, do not support this explanation because we are confident that our swap-equilibrated systems must be close to the global thermodynamic equilibrium in a wide T-range including $T \geq 0.2$ as argued in Ref. 10. If so, what could possibly be the reason for the Δ-shift effect? We see two possibilities: (i) it could be due to a systematic discrepancy between theory and simulations at higher q's (recall that the theory is valid up to a relative correction of $\mathcal{O}(q\bar{b})^2$), (ii) or it is simply due to stochastic variations of $\theta(q)$ (cf. eq. 90) within the ensemble. Below we show that the lion's share of Δ seems to be due to the second effect. To find the shift $\Delta(q)$ we apply (the inverse s-transform of) eq. 93 in the most relevant long-time regime, $t > 2\tau_L$:

$$\Delta(q) = \theta(q) - \theta_{\text{th}}(q) \tag{94}$$

where $\theta(q)$ is the long-time plateau of $C_2(q,t)$ corresponding to the low$-s$ limit of $C_2(q,s)$ (cf. the lhs of eq. 93), and $\theta_{\text{th}}(q)$ is the theoretical prediction for $\theta(q)$ corresponding to the rhs of eq. 75 at low s. More precisely,

$$\theta(q) \equiv \left\langle \frac{V}{T} \left| \bar{\sigma}_{22}(\underline{q}) \right|^2 \right\rangle = \frac{2}{(\Delta t_{\max})^2} \int_0^{\Delta t_{\max}} C_2(q,t)\,(\Delta t_{\max} - t)\,\mathrm{d}t \tag{95}$$

(cf. eq. 90) where $\langle ... \rangle$ brackets here mean averaging over many (m) independent systems and N_q independent orientations of $\underline{q}$ (with the same $|\underline{q}|$). Similar relations involving the volume- and time-averaged shear stress have been employed in Refs. 5, 9, and 12. The mean stress $\bar{\sigma}$ is defined as[51]

$$\bar{\sigma}_{22}(\underline{q}) = \frac{1}{\Delta t_{\max}} \int_0^{\Delta t_{\max}} \sigma_{22}(\underline{q},t)\mathrm{d}t \tag{96}$$

The working definition of $\theta_{\text{th}}(q)$ is given by the rhs of eq. 95 with the only change: the simulation-based $C_2(q,t)$ there should be replaced with the theoretical $C_{2\text{th}}(q,t)$ defined as the inverse s-transform of the rhs of eq. 75. Our analysis shows (see the previous point) that for $t > 2\tau_L$ the function $C_{2\text{th}}(q,t)$ can be approximated with eq. 92, so we get in analogy with eq. 95:[56]

$$\theta_{\text{th}}(q) \simeq \frac{2}{(\Delta t_{\max})^2} \int_0^{\Delta t_{\max}} 4G(t) \left[1 - \frac{G(t)}{K_{TL}(t)} \right] (\Delta t_{\max} - t)\,\mathrm{d}t \tag{97}$$

Thus, the theoretical $\theta_{\text{th}}(q)$ is actually predicted to be nearly independent of q for small q, $q\bar{b} \ll 1$. Obviously θ_{th} is closely related to μ_{sf} (cf. eq. 18 in Ref. 10), and, in any case, θ_{th} is independent of any quenched stress, either at $q = 0$ or at $q > 0$ (recall that the latter property is inherent in both $G(t)$ and $K_{TL}(t)$ as defined in eqs. (2) and (16) of Ref. 10). It is therefore likely that the statistical

fluctuations of $\theta(q)$ and $\theta_{\rm th}$ within the ensemble are independent. As a result we can write (cf. eq. 94):

$$\mathrm{var}(\Delta(q)) \simeq \mathrm{var}(\theta(q)) + \mathrm{var}(\theta_{\rm th}) \tag{98}$$

for any chosen q and T. Here $\mathrm{var}(\theta(q))$ is the variance of $\theta(q)$ averaged over the ensemble of m independent systems and N_q orientations of $\underline{q}$. Assuming Gaussian statistics of $\bar{\sigma}_{22}(\underline{q})$ (cf. ref. 9), it is easy to show that the relative standard deviation of $\left|\bar{\sigma}_{22}(\underline{q})\right|^2$ is just 1, which means that the relative standard deviation of $\theta(q)$ (which is averaged over mN_q independent values) is

$$\delta\theta(q)/\theta(q) \approx 1/\sqrt{mN_q} \tag{99}$$

where $\delta\theta(q) = \sqrt{\mathrm{var}(\theta(q))}$ (here we also used the natural property that $\bar{\sigma}_{22}(\underline{q})$ for different wave-vectors $\underline{q}$ are not correlated). The rhs of the above equation for $m = 100$ and $N_q = 2$ (valid for $0.2 \leq T \leq 0.3$ and all q's we considered) is $1/\sqrt{mN_q} \approx 0.071$. Furthermore, taking into account that $K_{TL}(t)$ is nearly constant at long t and low temperatures, $T \leq 0.24$, with $K_{TL}/G \gtrsim 5$, and using eq. 97 we estimate the relative standard deviation of $\theta_{\rm th}$ as

$$\delta\theta_{\rm th}/\theta_{\rm th} \sim \frac{1}{\sqrt{m}} \frac{\delta\mu_{sf}}{\mu_{sf}} \tag{100}$$

where the shear modulus μ_{sf} and its standard deviation $\delta\mu_{sf}$ have been calculated at different temperatures in ref. 10. It is more convenient to consider the ratio $X(q) \equiv \Delta(q)/\theta_{\rm th} = \theta(q)/\theta_{\rm th} - 1$ as a variable of interest. Taking into account that both $\delta\theta(q)/\theta(q)$ and $\delta\theta_{\rm th}/\theta_{\rm th}$ are small and that $\theta(q) \approx \theta_{\rm th}$, we get (based on eqs. 98)

$$\delta(\Delta(q)/\theta_{\rm th}) \approx \left[(\delta\theta(q)/\theta(q))^2 + \left(\delta\theta_{\rm th}/\theta_{\rm th}\right)^2\right]^{1/2} \tag{101}$$

Finally, we take into account a systematic difference between $\theta(q)$ and $\theta_{\rm th}$ leading to a non-zero $X_{\rm sys}(q) = \langle X \rangle$. Thus we get

$$\left\langle X^2 \right\rangle \approx \left(X_{\rm sys}(q)\right)^2 + \left(\delta(\Delta(q)/\theta_{\rm th})\right)^2 \tag{102}$$

We then calculated the average $\left\langle X^2 \right\rangle$ based on the simulation results for $q = q_{\rm min}$, $T = 0.2$, 0.21, 0.22, 0.23, 024: this way we get the root-mean-square (RMS) of X, $\mathrm{RMS}\left(\Delta(q)/\theta_{\rm th}\right) \approx 0.092$. On the other hand, the similar RMS average of $\delta(\Delta(q)/\theta_{\rm th})$, calculated using eqs. 99, 100, 101 is $\delta(\Delta(q)/\theta_{\rm th}) \approx 0.08$ which is close to $\delta\theta(q)/\theta(q) \approx 1/\sqrt{mN_q}$. It means that the systematic term X_{sys} is relatively small, and that the observed Δ can be largely explained by the inevitable statistical

error due to a random distribution of $\bar{\sigma}_{22}(\underline{q})$. Considering, in addition, all (T,q) combinations with $n_{q2} = \left(q/q_{\min}\right)^2 = 8,\ 32,\ 64$ and $T = 0.24$, 0.2 (cf. Figs. 6, 7) we get RMS $\left(\Delta/\theta_{\rm th}\right) \approx 0.086$, that is a smaller deviation which is closer to the lower bound of RMS(X), $1/\sqrt{mN_q} \approx 0.071$ (the fact that RMS$(X) \geq 1/\sqrt{mN_q}$ follows from eqs. 99, 101, 102).[57]

These results clearly show that the systematic deviation $X_{\rm sys}$ is not resolved here (it is masked by the stochastic part of $X = \Delta/\theta_{\rm th}$): were $X_{\rm sys}$ mattered, its effect would increase with q, while we detected an opposite trend. Therefore, the vertical shift Δ seems to be mostly a stochastic effect due a limited size of the ensemble.

12. As mentioned in section III B (see also Refs. 6 and 21) the four stress correlation functions analyzed in the present paper define the full time-space resolved tensorial stress correlation function, $C_{\alpha\beta\alpha'\beta'}(\underline{q},t)$, eq. 69, for 2D systems (cf. eq. (24) in Ref. 6):

$$C_{\alpha\beta\alpha'\beta'}(\underline{q},t) = \left(C_2(q,t) - 2C_s(q,t)\right)\delta_{\alpha\beta}\delta_{\alpha'\beta'} + \left(C_\perp(q,t) - C_2(q,t) + 2C_s(q,t)\right)\times$$
$$\left(q_\alpha q_\beta \delta_{\alpha'\beta'} + q_{\alpha'} q_{\beta'} \delta_{\alpha\beta}\right)/q^2 + C_s(q,t)\left(\delta_{\alpha\alpha'}\delta_{\beta\beta'} + \delta_{\alpha\beta'}\delta_{\beta\alpha'}\right) +$$
$$\left(C_\parallel(q,t) + C_2(q,t) - 2C_\perp(q,t) - 4C_s(q,t)\right) q_\alpha q_\beta q_{\alpha'} q_{\beta'}/q^4 \qquad (103)$$

In particular, the autocorrelation function of the shear stress (in the fixed coordinate frame, x,y) is[6,21]

$$C_{xyxy}(\underline{q},t) = C_s(q,t) + \left(C_\parallel(q,t) + C_2(q,t) - 2C_\perp(q,t) - 4C_s(q,t)\right) q_x^2 q_y^2/q^4 \qquad (104)$$

The above eqs. 103 and 104 are exactly valid provided that the system is perfectly isotropic. We have already established[10] that bulk properties of our pLJ systems are isotropic to a high precision at $T > T_f \approx 0.16$ after statistical averaging over a large ensemble. A similar statement concerning the wave-vector $\underline{q}$ (or distance $\underline{r}$) correlation functions is less trivial because here the finite box size (FBS) and the periodic boundary conditions (PBC) can affect correlation functions at large r or low q. We defer to a separate publication a discussion of these and related effects for the stress correlation functions resolved in real and $\underline{q}$-space. Here, instead, we limit the discussion to the results for an *extended* ensemble including (in addition to the original independent configurations) also the 'rotated configurations' obtained by turning the simulation box as a whole over an angle ϕ with uniform distribution of ϕ from 0 to 360°. Such an extended ensemble is perfectly isotropic by construction (that is, all directions are statistically equivalent there), so eqs. 103 and 104 are mathematically exact for it. Obviously, if some anisotropies (like preferential orientation of vectors connecting neighboring particles along the box sides) were present in the original configurations,

they get wiped out by the angular averaging implied by the extended sampling. Note, however, that the functions $C_s(q,t)$, $C_2(q,t)$, etc. are obtained here by averaging the corresponding stress correlators over all possible orientations of the wave-vector $\underline{q}$ (for a given $|\underline{q}|$), hence they remain the same for the extended ensemble.

At sufficiently long time, $t \gtrsim 2\tau_L$, the only surviving correlation is $C_2(q,t)$. At $T < T_g$ the function $C_2(q,t)$ shows a long-time slowly decaying tail which is nearly independent of q (cp. Figs. 4(d), 6(a), (b) and (c)). Therefore our direct simulation data point to a non-analytical q-dependence of the shear stress correlation function at long times (and small q) according to $C_{xyxy}(\underline{q},t) \propto q_x^2 q_y^2/q^4$, which indicates that correlations of shear stress in real space are long-range (see below). Moreover, using the theoretical eqs. 75, 92 we can predict the time-dependence of the shear-stress correlations (for $t \gtrsim 2\tau_L$) based on the bulk relaxation moduli:

$$C_{xyxy}(\underline{q},t) \approx 4G(t)\left[1 - \frac{G(t)}{K_{TL}(t)}\right] q_x^2 q_y^2/q^4 \tag{105}$$

Doing its inverse Fourier transform to real space (cf. Refs. 6, 20, and 21) we get for $r \ll L$ (the latter condition is needed to avoid the FBS effects):

$$C_{xyxy}(\underline{r},t) \approx -\frac{1}{\pi}\frac{1}{r^2}\cos(4\theta)G(t)\left[1 - \frac{G(t)}{K_{TL}(t)}\right], \;\; t \gg \tau_L \sim \frac{2\rho}{\eta_L} r^2 \tag{106}$$

where θ is the polar angle between the distance vector $\underline{r}$ and the x-axis. It means that for any t, $\tau_v \ll t \lesssim \tau_\alpha$, there is a wide range of distances where the $1/r^2$ power law, eq. 106, is valid (recall that τ_v is the microscopic time for particle velocity relaxation by collisions and vibrations). This result is in harmony with the theories[6,20,21] predicting the $1/r^d$ power-law stress-correlation tail for isotropic glass-forming liquids. Note that strictly speaking eq. 106 is justified here for an extended ensemble described above.

13. In the present study we neglected a q-dependence of the generalized shear relaxation modulus $G(q,t)$, cf. eq. 19. By contrast, some theoretical and simulation studies[25,40–43] report a rather significant q-dependence of $G(q,t)$. There are two main reasons for this effect: (i) It is present in polymer systems[25,40,43] where it is simply due to a large size of macromolecular coil: the size $\bar{b}$ is then $\bar{b} = R_{coil} \gtrsim \sqrt{N_m} l_m$, where $N_m \gg 1$ is the polymerization degree and l_m is monomer size. (ii) It was also detected in glass-forming liquids near the glass transition, T_g.[41–43] More precisely, they considered a q-dependence of the generalized shear viscosity $\eta(q)$ which is related to $G(q,t)$: $\eta(q) = \int_0^\infty G(q,t)\mathrm{d}t$ (cf. eq. 87). Quite naturally they found[41–43] that $\eta(q)$ becomes significantly lower than $\eta(0)$ (say, by a factor of 2) at sufficiently large $q \sim 1/\xi_\eta$, where ξ_η is the

viscosity-based correlation length. Still, at lower q's, $q\xi_\eta \ll 1$, the q-dependence of $\eta(q)$ can be neglected. The simulation studies[41,42] deal with a 3D binary mixture of soft spheres and show that the length $\xi_\eta \sim b_m/3$ (b_m is molecular size) is low well above T_g, but it increases to $\xi_\eta \sim 4b_m$ on cooling below T_g. Simulations of liquid butane[43] reveal a similar trend with $\xi_\eta/b_m \sim 3 \div 5$. We emphasize that the systems studied in refs. 41–43 are quite different from our system which is both polydisperse and two-dimensional. To assess the q-dependence of $G(q,t)$ for our system we chose to consider the correlation function $C_2(q,t)$ well below the glass transition, at the lowest $T = 0.2$ (where the q-effect is expected to be stronger). In this regime $C_2(q,t)$ shows a long-time plateau, $C_2(q,t) \approx \theta(q)$ (cf. eq. 90) which, by virtue of eq. 75, is related to the plateau levels, $G_s(q)$ and $K_s(q)$ of $G(q,t)$ and $K(q,t)$, respectively: $\theta(q) \approx 4G_s(q)\,[1 - G_s(q)/K_s(q)]$ (cf. eq. 91). Therefore, the q-dependence of θ is expected to provide an idea on the behavior of the long-time shear relaxation modulus. Somewhat surprisingly, our simulation data point to $\theta(q) \approx 45$ which is nearly independent of q in a rather wide q-range, for $q\bar{b} < 2.5$ (recall that the data considered in the present paper correspond to a more narrow range, $q\bar{b} < 0.5$). Furthermore, we found that $G(q,t)$ at $t = 0$ also stays virtually independent of q for $q\bar{b} < 0.5$ (this conclusion is based on the stress-correlation data and the exact relation, $G(q,t) = C_s(q,t)$ at $t = 0$, which comes from eq. 70). Thus, for the 2D pLJ system considered here we do not observe any indication of a q-dependence of $G(q,t)$ in the studied q-range, $q\bar{b} \lesssim 0.5$. This statement is also backed by a very good agreement between the shear stress correlation function $C_s(q,t)$ obtained by simulations and its theoretical prediction based on the exact eq. 70 and involving the approximation $G(q,t) \approx G(t)$ (cf. Figs. 4 - 7).

V. SUMMARY AND CONCLUSIONS

1. In the present paper we analyzed spacio-temporal correlations of mechanical stress and other variables both theoretically and by MD simulations of a two-dimensional polydisperse system of LJ particles (2D pLJ) described in Appendix A. The theory is based on the FDT relations, eqs. 62, 70, 71, 72, 75, between the wave-vector ($\underline{q}$) dependent correlation functions and the generalized relaxation moduli, $G(q,t)$ and $K(q,t)$, for shear and longitudinal stress, respectively. We argue that at low q (when the wave-length $\lambda = 2\pi/q$ strongly exceeds the particle size $\bar{b}$) the modulus $G(q,t)$ can be approximated with the classical bulk shear relaxation modulus $G(t)$, that is, a q-dependence of $G(q,t)$ can be neglected at low q (cf. section II C). By contrast, we show that a

similar approximation for the longitudinal modulus, $K(q,t)$ (which was adopted before[6,20,21]) is not valid in practice since the bulk modulus $K(0,t) = K_L(t)$ is not universal: it depends on the thermostat employed in simulations[10], hence $K(q,t)$ may be discontinuous at $q = 0$ (cf. section II C). To overcome this issue a theoretical approach was developed (cf. section II D) which allows to obtain $K(q,t)$ in terms of the bulk modulus $K_L(t)$, bulk correlation functions of energy and pressure, the particle MSD, $h_0(t)$, the static structure factor $S(q)$ and the heat conductivity κ. Our theory is akin to the generalized hydrodynamic approach[38,47].

2. We elucidate that the generalized longitudinal modulus $K(q,t)$ at $q \to 0$ cannot be uniformly approximated by a function of time only, and so, in particular, $\lim_{q\to 0}\lim_{t\to\infty} K(q,t) < \lim_{t\to\infty}\lim_{q\to 0} K(q,t)$. Moreover, in polydisperse systems the first limit can be much smaller than the second, and none of these limits is related to the isothermic bulk compressibility of the system. The time dependence of $K(q,t)$ for a low q above T_g is illustrated in Fig. 8. It involves a strong decrease of $K(q,t)$ at short times, $t \lesssim \tau_v$ (with τ_v, the vibration/collision time), due to an initial relaxation of the system structure and particle velocities, a further structural relaxation (at nearly constant energy density) followed by an adiabatic shoulder (quasi-plateau), then a further decrease of $K(q,t)$ due to heat transport with characteristic time $\tau_T = n_0 c_{vs}/\left(\kappa q^2\right)$ defined by the thermal conductivity κ and wavevector q (the thermal diffusion stage). The thermal process is followed by the isothermic shoulder with $K(q,t) \approx K_{TL}(t) \approx K_{TLs}$, and the terminal relaxation by particle interdiffusion leading a significant decrease of $K(q,t)$ from the bulk longitudinal isothermic modulus K_{TL} to the equilibrium level $K(q,\infty) = n_0 T/S(q)$ defined by the static structure factor $S(q)$. The characteristic time of the latter process is $\tau_{inter} = 1/\left(D_{inter} q^2\right)$, where the interdiffusion constant D_{inter} is close to the particle self-diffusivity D_s (for the 2D pLJ system we studied, see Appendix A).

3. The terminal interdiffusion stage for $K(q,t)$ is clearly reflected in the dynamical structure factor, $S(q,t)$, for $T = 0.3$ shown in Fig. 3. This figure also demonstrates a very good agreement between the direct simulation data for $S(q,t)$ and the theoretical results based on the predicted $K(q,t)$ and the general relation, eq. 62. The proposed theoretical approach to calculate $K(q,t)$ is thus validated numerically. It is noteworthy that well below T_g the structure factor $S(q,t)$ exhibits a long-time plateau, $S(q,t) \approx S(q) - n_0 T/K_{TLs}$ for $t \gtrsim 2\tau_L$ (see Fig. 9), which corresponds to the isothermic quasi-plateau of the longitudinal modulus, $K(q,t) \approx K_{TLs}$ (this plateau occurs before the interdiffusion stage which is not visible since the sampling time $\Delta t_{\max} \ll \tau_{inter}$). The long-time plateau of $S(q,t)$ is related to the polydispersity of the studied system, as discussed in Ref. 36.

4. The obtained theoretical longitudinal modulus $K(q,t)$ was used to predict all components of the stress correlation tensor, $C_{\alpha\beta\alpha'\beta'}(\underline{q},t)$, based on the general relations, eqs. 70, 71, 72, 75. The results are compared with our simulation data on the 2D pLJ system in Figs. 4, 5, 6, 7. Most of the predicted results are in excellent agreement with the simulation data for $q/q_{\min} \leq 8$, i.e. $q\bar{b} \lesssim 0.5$ (see Figs. 4, 5, 6). The agreement gets slightly worse well below the glass transition temperature T_g for the highest q's we studied.

5. The theoretical approach to calculate the time-space resolved stress correlations[6,20,21] was developed for the monodisperse isothermal systems (with infinite thermal conductivity κ). In the present paper the theory is generalized to the case of a polydisperse system with finite κ. The generalized theory we developed is asymptotically exact for $q \to 0$; at finite q it works within a relative error of $\mathcal{O}(q\bar{b})^2$.

6. As demonstrated in Figs. 4, 5, 6, 7, the basic stress-correlation functions, C_s, $C_\parallel$, $C_\perp$, vanish beyond the sound attenuation time τ_L. By contrast, the autocorrelation function of the transverse normal stress, $C_2(q,t)$, shows a shoulder at $t > \tau_L$ near and below T_g (the shoulder transforms to a plateau well below T_g). As discussed in section IV this feature leads to long-range dynamical correlations of the local shear stress $\sigma_{xy} = \sigma_{xy}(\underline{r})$ according to the power law, $1/r^2$ for 2D systems (where $r = |\underline{r}_1 - \underline{r}_2|$ is the distance between two points) in agreement with theoretical[6,20,21] and simulation[22,23] results. Note that this power law is justified in the present paper for an extended ensemble described in point 12 of section IV. The long-range correlations characterize the (transiently) quenched stress field in a glassy system.

7. The plateau of $C_2(q,t)$ persists until $t \sim \tau_\alpha$. Interestingly, our stress correlation data indicate that the terminal relaxation of $C_2(q,t)$ gets slower at higher q's, $q\bar{b} \gtrsim 0.5$, with relaxation time longer than τ_α based on $G(t)$. This effect becomes stronger as q increases up to $q\bar{b} \sim 2$.

8. Below the glass transition, $T < T_g$, we detected a small discrepancy between the predicted $C_2(q,t)$ (cf. the rhs of eq. 75) and the direct simulation data on C_2. This discrepancy, $\Delta(q)$, takes positive or negative values depending on T and q. However, as we demonstrated numerically (cf. point 11 of the Discussion), its relative root-mean-square value (denoted as $\mathrm{RMS}(\Delta(q)/\theta_{\mathrm{th}})$) is largely accounted for by the statistics of the time-averaged quenched stress whose relative dispersion is defined by the size of the statistical ensemble. Therefore, the vertical shift Δ is mostly a stochastic effect due a limited size of the ensemble, which is constant for the considered temperature range. Other contributions to the $\mathrm{RMS}(\Delta(q)/\theta_{\mathrm{th}})$, including that due to the systematic error of the predicted $C_2(q,t)$, appear to be small. We anticipate, however, that the latter (systematic)

contribution may become significant for large wave-vectors ($q/q_{\min} \gg 8$).

Conflicts of interest

There are no conflicts of interest to declare.

ACKNOWLEDGMENTS

A grant of computer time at the HPC computing cluster of the University of Strasbourg is gratefully acknowledged. L.K. was supported by a doctoral contract from the University of Strasbourg in the framework of the IRTG "Soft Matter Science".

Appendix A: 2D pLJ system and simulation algorithm

We study a 2-dimensional (2D) system of polydisperse Lennard-Jones (pLJ) particles with the same mass m.[10,11,17,36,48] The particle diameters are uniformly distributed around the mean diameter $\bar{b}$, between $0.8\bar{b}$ and $1.2\bar{b}$. The particle size polydispersity index is $\overline{b^2}/\bar{b}^2 - 1 \approx 0.013$. Each pair of particles ($l = (a,a')$) interacts with the energy $u_{LJ}(s = r/b_l)$, where the interaction range b_l is defined by the Lorentz rule, $b_l = (b_a + b_{a'})/2$, and the LJ potential $u_{LJ}(s) = 4\varepsilon\left(s^{-12} - s^{-6}\right)$ was truncated at $s_{cut} = 2^{7/6}$ and shifted to avoid discontinuity at $s = s_{cut}$. All quantities are given in LJ units: m, $\bar{b}$, ε and the Boltzmann constant k_B are set to 1.

We used the standard molecular dynamics (MD) simulations (velocity-Verlet algorithm with MD time-step $t_{\mathrm{MD}} = 0.005$) with periodic boundary conditions as implemented in the LAMMPS code.[49] The system of $N = 10^4$ particles was first tempered well in the liquid regime, at constant temperature $T_0 = 1$ and pressure $p_0 = 2$ using the Nosé-Hoover thermostat and barostat to prepare $m = 100$ well-equilibrated independent configurations which were then continuously cooled down with rate $\mathrm{d}T/\mathrm{d}t = -10^{-5}$ at $p_0 = 2$. These slow cooling runs allowed us to estimate the dilatometric glass-transition temperature, $T_g \approx 0.26$, in agreement with the previous studies[17].

To better equilibrate the quenched configurations at $T \leq 0.5$ we used a hybrid approach involving Monte-Carlo (MC) dynamics. The MC part involves a combination of local particle displacements and non-local particle swaps.[52] The system volume fluctuations (controlled by an MC barostat[53] to impose $p_0 = 2$) were allowed as well. This way an ensemble of m independent configurations ($m = 100$ for $0.2 \leq T \leq 0.3$, $m = 50$ for $T > 0.3$, $m = 20$ for $T < 0.2$) was tempered over 10^7 MC steps at constant pressure. Then the instantaneous volume was fixed and the system

equilibrated further at constant volume over 10^7 MC steps (with local and swap moves), and over the same time with local moves only. This MC approach was successful in equilibrating the pLJ system below T_g, down to $T_f = 0.16$ below which particle demixing occurs.[10] Each configuration was then tempered for $2 \cdot 10^5$ LJ time units with MD Nosé-Hoover (NH) dynamics at constant pressure $p_0 = 2$ to equilibrate the velocities, and then over the same time at constant volume.

Finally, the production runs (served to obtain all correlation functions) were performed in the NVT ensemble during the total sampling time $\Delta t_{\max} = 10^5$. The time space between the data entries was $\delta t = 0.2$ for q-dependent variables, and $\delta t = 0.05$ for all other variables. The thermal mass parameter Q of the NH thermostat was $Q = 10T/3$ corresponding to a high Nosé frequency $\omega_Q = (2TNd/Q)^{1/2} \sim 110$ and a short thermostat relaxation time (the Nosé time) $\tau_{damp} = \sqrt{2}/\omega_Q \ll \delta t$. The linear dimension of the simulation box is $L \sim 100$, the system volume $V = L^2$, and the mean concentration $n_0 = N/V \sim 1$ in all the cases.

Appendix B: Temperature autocorrelation function and the heat conduction coefficient

The $q-$dependent temperature autocorrelation function can be defined as

$$C_T(\underline{q},t) = \frac{N}{T^2}\left\langle \delta T_{\underline{q}}(t+t')\delta T_{-\underline{q}}(t')\right\rangle \tag{B1}$$

where $\langle ...\rangle$ imply the ensemble and time-shift averaging (over t'), and

$$\delta T_{\underline{q}}(t) = T_{\underline{q}}(t) - \left\langle T_{\underline{q}}(t)\right\rangle,\ T_{\underline{q}}(t) = \frac{1}{N}\sum_a \delta T_a(t)\exp\left(-\mathrm{i}\underline{q}\cdot\underline{r}_a(t)\right) \tag{B2}$$

is a Fourier component of the temperature fluctuation field (the index a runs over all particles). Here

$$\delta T_a(t) = m_a \underline{v}_a(t)^2/d - T_0 \tag{B3}$$

is the excess kinetic temperature of particle a, T_0 is the mean temperature of the system (which is prescribed by the thermostat), and d is the space dimension. Note that $\langle \delta T_a(t)\rangle = 0$ and $\left\langle T_{\underline{q}}(t)\right\rangle = 0$, hence $\delta T_{\underline{q}}(t) = T_{\underline{q}}(t)$ for $q \neq 0$. Note also a direct way to calculate $C_T(\underline{q},t)$ based on simulation data:

$$C_T(\underline{q},t) = \frac{1}{NT_0^2}\sum_{a,a'}\left\langle \delta T_a(t+t')\delta T_{a'}(t')\exp\left(-\mathrm{i}\underline{q}\cdot\left(\underline{r}_a(t+t') - \underline{r}_{a'}(t')\right)\right)\right\rangle \tag{B4}$$

which is analogous to the standard definition of the dynamical structure factor $S(\underline{q},t)$ (see eq. 61).

By virtue of the FDT (i.e., the linear response theory[3]) the correlation function C_T is related to the temperature response $\Delta T_{\underline{q}}(t) = T_{\underline{q}}(t) - T_{\underline{q}}(0^-)$ induced by a heat wave generated by the following perturbation of particle velocities applied at $t = 0$ (cf. eq. 4):

$$\underline{v} \to \underline{v}\left(1 + \exp\left(\mathrm{i}\underline{q}\cdot\underline{r}\right)\varepsilon_v/d\right) \tag{B5}$$

Namely,

$$\Delta T_{\underline{q}}(t)/\varepsilon_v = TC_T(q,t), \;\; t > 0 \tag{B6}$$

where $T = T_0$ and $\varepsilon_v \to 0$. Using the above equation one immediately gets

$$C_T(q,0^+) = 2/d \tag{B7}$$

The time dependence of C_T can be obtained for low q's using the generalized hydrodynamic approach (cf. section II D). The longitudinal pressure increment we get (cf. eq. 31):

$$\Delta p_{xx}(s) = K_{AL}(s)\varepsilon(s) + \chi(s)h(s) \tag{B8}$$

where $\varepsilon_{xx} = -\varepsilon$ is the longitudinal strain eventually generated by the initial heat wave, and $h = h_i + h_t$ is the heat per particle including the initial heat $h_i = \varepsilon_v T$ injected in the system at $t = 0$ (as follows from eq. B5) and the heat h_t transferred into a cell by thermal conductivity. Note that here, as before, we assume that the wave-vector $\underline{q}$ is oriented along the x-axis, and the phase factor $e^{\mathrm{i}qx}$ is omitted. The time-dependence of h_t is given by eq. 32, where the temperature increment ΔT is (cf. eq. 36):

$$\Delta T(s) = \frac{T}{n_0}\chi(s)\varepsilon(s) + \frac{h(s)}{c_v(s)} \tag{B9}$$

Another relation defining the strain $\varepsilon = \varepsilon(t)$ in terms of pressure p_{xx} is given by two equations corresponding to mass and momentum conservation:

$$\frac{\partial n}{\partial t} = -\nabla\cdot\underline{j}, \;\; mn_0\frac{\partial v_x}{\partial t} = -\frac{\partial p_{xx}}{\partial x} = -\mathrm{i}q\Delta p_{xx} \tag{B10}$$

where $n = n(x,t) = n_0(1+\varepsilon(t)e^{\mathrm{i}qx})$ and $\underline{j} = n\underline{v} \simeq n_0\underline{v}$. Using the above equations we find $\Delta T(s) \equiv \Delta T_{\underline{q}}(s)$ and finally, on using eq. B6, the s-transform of $C_T(q,t)$:

$$C_T(q,s) = \left[c_v(s) + \frac{\kappa q^2}{n_0 s} + \frac{T}{n_0}\frac{p_T(s)^2}{K_{TL}(s) + mn_0 s^2/q^2}\right]^{-1} \tag{B11}$$

This equation agrees with eq. (18) of Ref. 54 provided that the bulk modulus K_B there is identified with the isothermic longitudinal modulus (K_{TL}). Eq. B11 can be also obtained in a simpler heuristic way following the approach outlined in point 2 of the Discussion.

The time-dependence of $C_T(q,t)$ obtained directly from our simulation data typically shows a decay superimposed with decaying oscillations. Such a behavior also follows from eq. B11. Doing inverse s-transform and applying approximations similar to those that led to eq. 47 we obtain

$$C_T(q,t) \approx \frac{1}{c_{pL}(t)} \left\{ (r(t)-1)\cos\left(\omega(t)t\right)\exp\left(-q^2 t\Gamma(t)\right) + \exp\left(-q^2 t \frac{\kappa}{n_0 c_{pL}(t)}\right)\right\} \qquad \text{(B12)}$$

where

$$c_{pL}(t) \approx c_v(t) r(t),\ r(t) = K_{AL}(t)/K_{TL}(t),$$

$$\omega(t) \approx \left[\frac{K_{AL}(t)}{mn_0}\right]^{1/2},\ \Gamma(t) \approx \frac{1}{2mn_0}\int_0^t \left[K_{AL}(t') - K_{AL}(t)\right] \mathrm{d}t'$$

Here $c_{pL}(t)$ is the heat capacity at constant longitudinal normal pressure p_{xx} and constant transverse area (i.e. at no deformation in the plane perpendicular to the x-axis, cf. eq. 77). Note that eq. B12 at $t = 0$ agrees with eq. B7 since $c_v(t=0) = d/2$.[11]

Eq. B12 for $C_T(q,t)$ was used to obtain the thermal conductivity κ at different temperatures by fitting it to the simulation data (the approximations like $c_v(t) \approx c_{v0}(t)$, valid because the relevant time is sufficiently long, $t \gg \tau_{damp}$, were used to this end). The results are quoted in section II E.

DATA AVAILABILITY

The data that support the findings of this study are available from the corresponding author upon reasonable request.

REFERENCES

[1] M. Fuchs, Adv. Polym. Sci. **36**, 55 (2010).

[2] A. Nicolas, E.E. Ferrero, K. Martens, and J.-L. Barrat, Rev. Mod. Phys. **90**, 045006 (2018).

[3] J. P. Hansen and I. R. McDonald, *Theory of Simple Liquids*, Academic Press, NY, 2006.

[4] D. Forster, *Hydrodynamic Fluctuations, Broken Symmetry, and Correlation Fluctuations*, Benjamin Cummings, London, 1983.

[5] I. Kriuchevskyi, J. P. Wittmer, H. Meyer, O. Benzerara and J. Baschnagel, *Phys. Rev. E*, 2018, **97**, 012502.

[6] L. Klochko, J. Baschnagel, J. P. Wittmer and A. N. Semenov, *Soft Matter*, 2018, **14**, 6835.

[7] J. P. Wittmer, H. Xu, P. Polińska, F. Weysser and J. Baschnagel, *J. Chem. Phys.*, 2013, **138**, 12A533.

[8] J. P. Wittmer, H. Xu, O. Benzerara and J. Baschnagel, *Mol. Phys.*, 2015, **113**, 2881.

[9]L. Klochko, J. Baschnagel, J. P. Wittmer and A. N. Semenov, *J. Chem. Phys.*, 2019, **151**, 054504.

[10]L. Klochko, J. Baschnagel, J. P. Wittmer and A. N. Semenov, *Soft Matter*, 2021, **1**7, 7867.

[11]L. Klochko, J. Baschnagel, J. P. Wittmer and A. N. Semenov, *J. Chem. Phys.*, 2021, **154**, 164501.

[12]G. George, L. Klochko, A. N. Semenov, J. Baschnagel, and J. P. Wittmer, Eur. Phys. J. E **44**, 13 (2021).

[13]An alternative assumption is that the periodic boundary conditions (PBC) are applied.

[14]F. Vogel and M. Fuchs, Eur. Phys. J. E **43**, 70 (2020).

[15]M. Hassani, E.M. Zirdehi, K. Kok, P. Shall, M. Fuchs, and F. Varnik, EPL **124**, 18003 (2018).

[16]H. Xu, J. P. Wittmer, P. Polińska and J. Baschnagel, *Phys. Rev. E*, 2012, **86**, 046705.

[17]J. P. Wittmer, H. Xu, P. Polińska, F. Weysser and J. Baschnagel, *J. Chem. Phys.*, 2013, **138**, 191101.

[18]J. L. Lebowitz, J. K. Percus and L. Verlet, *Phys. Rev.*, 1967, **153**, 250.

[19]P. G. Debenedetti and F. H. Stillinger, *Nature*, 2001, **410**, 259.

[20]M.Maier, A.Zippelius, M.Fuchs, PRL 119, 265701 (2017).

[21]M.Maier, A.Zippelius, M.Fuchs, J.Chem.Phys. 149, 084502 (2018).

[22]A. Lemaître, *Phys. Rev. Lett.*, 2014, **113**, 245702.

[23]A. Lemaître, J.Chem.Phys. 2015, **143**, 164515.

[24]U. Balucani, M. Zoppi, Dynamics of the liquid state. Oxford Univ. Press, Oxford, 2003.

[25]A. N. Semenov, J. Farago, and H. Meyer, J. Chem. Phys. 136, 244905 (2012).

[26]Note that the condition 15 does not imply any jump of $\sigma_{\alpha\beta}(\underline{q},t)$ at $t=0^+$ if the center-of-mass velocity of the system is kept equal to 0.

[27]C. Ruscher, A. N. Semenov, J. Baschnagel and J. Farago, *J. Chem. Phys.*, 2017, **146**, 144502.

[28]L. D. Landau and E. M. Lifshitz, *Theory of Elasticity*, Pergamon Press, New York, 1959.

[29]E. B. Tadmor and R. E. Miller, *Modeling Materials*, Cambridge University Press, Cambridge, 2011.

[30]We do not use subscript 'L' in $K(q,t)$ since a q-dependent compression can be only longitudinal; it can be isotropic only for $q=0$.

[31]R. B. Bird, R. C. Armstrong and O. Hassager, *Dynamics of Polymeric Liquids: Fluid Mechanics*, Wiley, NY, 1987.

[32]M. P. Allen and D. J. Tildesley, *Computer Simulation of Liquids*, Oxford University Press, Oxford, 2017.

[33]Here and below the brackets $\langle ...\rangle$ mean ensemble average supplemented with the averaging over

t', and $\delta X \equiv X - \langle X \rangle$ for any $X = T(t)$, $p(t)$, etc.

[34]Simultaneous correlations corresponding to the time-shift $t = 0$ are not altered by the thermostat due to its canonical nature.

[35]Note that here we deal with nondimensional specific heat per particle, c_v, which is equal to the total heat capacity of the system divided by Nk_B.

[36]L. Klochko, J. Baschnagel, J. P. Wittmer, O. Benzerara, C. Ruscher and A. N. Semenov, *Phys. Rev. E*, 2020**, 102**, 042611.

[37]W.Götze, Complex Dynamics of Glass-Forming Liquids, a mode-coupling theory. Oxford Univ. Press, N.Y., 2009.

[38]W. Götze and A. Latz, J.Phys.:Condens.Matter 1, 4169 (1989).

[39]The glass-transition temperature $T_g \approx 0.26$ was determined in prior Monte Carlo (MC) and MD studies using a continuous cooling protocol with a (standard choice for the) finite cooling rate.[10] Therefore, T_g corresponds to the temperature where the α-relaxation time becomes comparable to the cooling time (in the MC simulations with local moves or MD simulations), and the system falls out of equilibrium. However, thanks to the particle-swap MC technique[52] we succeed in equilibrating our 2D pLJ system down to $T = 0.16$.[10] Starting from these equilibrated configurations we performed MD simulations to explore the equilibrium dynamics of the supercooled liquid, also below $T_g \approx 0.26$ (cf. Ref. 10 for a detailed discussion). Here we continue to report T_g as a relevant temperature for our model because for $T \lesssim T_g$ dynamic correlation functions show pronounced plateaux for times beyond the initial short-time relaxation. Upon cooling these plateaux increase in length and extend over the entire sampling time of the MD simulation at low T.

[40]R. M. Puscasu, B. D. Todd, P. J. Daivis, and J. S. Hansen, J. Chem. Phys. 133, 144907 (2010).

[41]A.Furukawa, H.Tanaka, PRL 103, 135703 (2009).

[42]A.Furukawa, H.Tanaka, Phys. Rev. E 84, 061503 (2011).

[43]R. M. Puscasu, B. D. Todd, P. J. Daivis, and J. S. Hansen, Phys. Rev. E **82**, 011801 (2010).

[44]Note that the agreement at long times slightly deteriorates at low temperatures, $T \lesssim T_g$, which is a natural effect of the poorer statistics in the regime of long structural relaxation time τ_α.

[45] Note that time dependence of heat capacity $c_v(t)$ can be neglected at $t \gtrsim \tau_T$.[36]

[46]The affine moduli μ_A and η_A are discussed in Ref. 10.

[47]L.P. Kadanoff and P.C. Martin, *Ann. Phys., NY* 1963, 24, 419.

[48]A. Tanguy, J. P. Wittmer, F. Leonforte and J.-L. Barrat, *Phys. Rev. B*, 2002, **66**, 174205.

[49]S. C. Plimpton, *Comput. Phys.* **117**, 1 (1995).

[50]More precisely, the rate $1/\tau_s$ is equal to the real part of the smallest root s of equation $\rho s^2/q^2 + G(q,-s) = 0$, cf. the denominator in the rhs of eq. 70: $1/\tau_s = \Re(s)$. In a similar way $1/\tau_L$ is defined by $\rho s^2/q^2 + K(q,-s) = 0$, cf. the denominator in the rhs of eq. 71.

[51] Both relations 96, 95 assume a virtual stationarity of a well-equilibrated system within a metabasin.

[52]A. Ninarello, L. Berthier and D. Coslovich, *Phys. Rev. X*, 2017, **7**, 021039.

[53]D. Frenkel and B. Smit, *Understanding Molecular Simulation*, Academic Press, London, 2002.

[54]P. Scheidler, W. Kob, A. Latz, J. Horbach, and K. Binder, Phys.Rev. B 63, 104204 (2001).

[55]Macroscopic isotropy of the studied systems was demonstrated in ref. 10.

[56]Note that the region $t \lesssim 2\tau_L$ provides a negligible contribution to the integral in eq. 97 since $\Delta t_{\max} \gg \tau_L$.

[57]Note that while $N_q = 2$ for all q's we consider (with $n_{q2} = 1, 8, 32, 64$), it typically gets higher for larger q.

[58]B. Illing, S. Fritschi, D. Hajnal, C. Klix, P. Keim and M. Fuchs, *Phys. Rev. Lett.*, 2016, **117**, 208002.

[59]The importance of interdiffusion processes for glass-forming systems with size polydispersity was discussed in Ref. 60, and for binary mixtures in the framework of mode-coupling theory in Ref. 61. However, the general form of the magnitude of the interdiffusion term (cf. prefactor in eq. 52) was not recognized there.

[60]P.N. Pusey, R.J.A. Tough, Adv. Coll. Interf. Sci. 16, 143 (1982).

[61]M.Fuchs and A.Latz, Physica A 201, 1 (1993).

[62]$K_T(t)$, $K_A(t)$ are universal functions by their definition implying a perfect temperature adjustment to keep constant either T or the entropy S. Therefore, $K_T(t)$ or $K_A(t)$ cannot be directly obtained by, say, simulations with imperfect thermostats (allowing for some undefined T-variations). Still they can be calculated even in this case based on the non-universal correlation functions, but it requires application of certain transformations to the correlation data as described in ref. 10. By contrast, this problem is absent for $G(q,t)$ since shear stress fluctuations

are insensitive to small T-variations.

FIGURE CAPTIONS

FIG. 1. Longitudinal relaxation modulus $K(q_{\min},t)$ for $T = 0.4,\ 0.3,\ 0.26,\ 0.24,\ 0.2$ calculated using eqs. 43, 45 (black curves from bottom to top) and its approximation, eqs. 47, 43 (red curves). Note that the black curves superimpose almost completely onto the corresponding red curves at $t \gtrsim 100$.

FIG. 2. Longitudinal modulus $K(q,t)$ (black curve), adiabatic modulus $K_{AL}(t)$ (red curve) and isothermic modulus $K_{TL}(t)$ (blue curve). Upper panel: $T = 0.4$, $q = q_{\min}$; lower panel: $T = 0.3$, $q = \sqrt{8}q_{\min}$.

FIG. 3. The dynamical structure factor $S(q,t)$ vs. t for $T = 0.3$, $q = q_{\min}$ (upper left panel), $T = 0.3$, $q = \sqrt{8}q_{\min}$ (upper right), $T = 0.26$, $q = q_{\min}$ (lower left), $T = 0.24$, $q = \sqrt{8}q_{\min}$ (lower right). Simulation results based on eq. 61 are shown with red curves; theoretical results, eqs. 68, 67 – black curves.

FIG. 4. Time dependence of correlation functions for shear stress, $C_s(q,t)$ (upper left panel); longitudinal stress, $C_{\parallel}(q,t)$ (upper right); normal stress cross-correlations, $C_{\perp}(q,t)$ (lower left); second normal stress, $C_2(q,t)$ (lower right) for $q = q_{\min} \equiv 2\pi/L$. Black curves – theory, red symbols and curves – simulation data. We show symbols only for short times ($t \leq 6$) for clarity. The temperature $T = 0.4$ (a), 0.3 (b), 0.26 (c), 0.24 (d), 0.2 (e).

FIG. 5. Same functions (as in Fig. 4) for $T = 0.3$ and $n_{q2} \equiv \left(q/q_{\min}\right)^2 = 8$ (a), $n_{q2} = 32$ (b), 64 (c).

FIG. 6. Same functions (as in Fig. 4) for $T = 0.24$ and $n_{q2} \equiv \left(q/q_{\min}\right)^2 = 8$ (a), $n_{q2} = 32$ (b), 64 (c). The theoretical data for C_2 are vertically shifted by $\Delta = 1.9$ for $n_{q2} = 32$, and $\Delta = 2$ for $n_{q2} = 64$.

FIG. 7. Same functions (as in Fig. 4) for $T = 0.2$ and $n_{q2} \equiv \left(q/q_{\min}\right)^2 = 8$ (a), $n_{q2} = 32$ (b), 64 (c). The theoretical data for C_2 are vertically shifted by $\Delta = 4.7$ for $n_{q2} = 8$, $\Delta = 1.2$ for $n_{q2} = 32$, and $\Delta = 1.13$ for $n_{q2} = 64$.

FIG. 8. The time dependence of $K(q_{\min},t)$, the generalized longitudinal modulus, at $T = 0.4$ showing all relaxation stages as described in the text.

FIG. 9. The dynamical structure factor $S(q,t)$ for $T = 0.2$, $q = q_{\min}$. Simulation results based on eq. 61 (red curve), theoretical results, eqs. 68, 67 (black curve). The blue horizontal line indicates the long-time isothermic plateau level $= S(q) - n_0 T / K_{TLs}$.

FIG. 10. The dynamical structure factor $S(q,t)$ based on simulation data (black line), its exponential approximation, eq. 52 (blue curve), and the correlation function of composition fluctuations, $1.33 S_{\psi}(q,t)$, obtained by simulations (red curve). $T = 0.4$ and $q = \sqrt{8} q_{min}$ for all the curves.

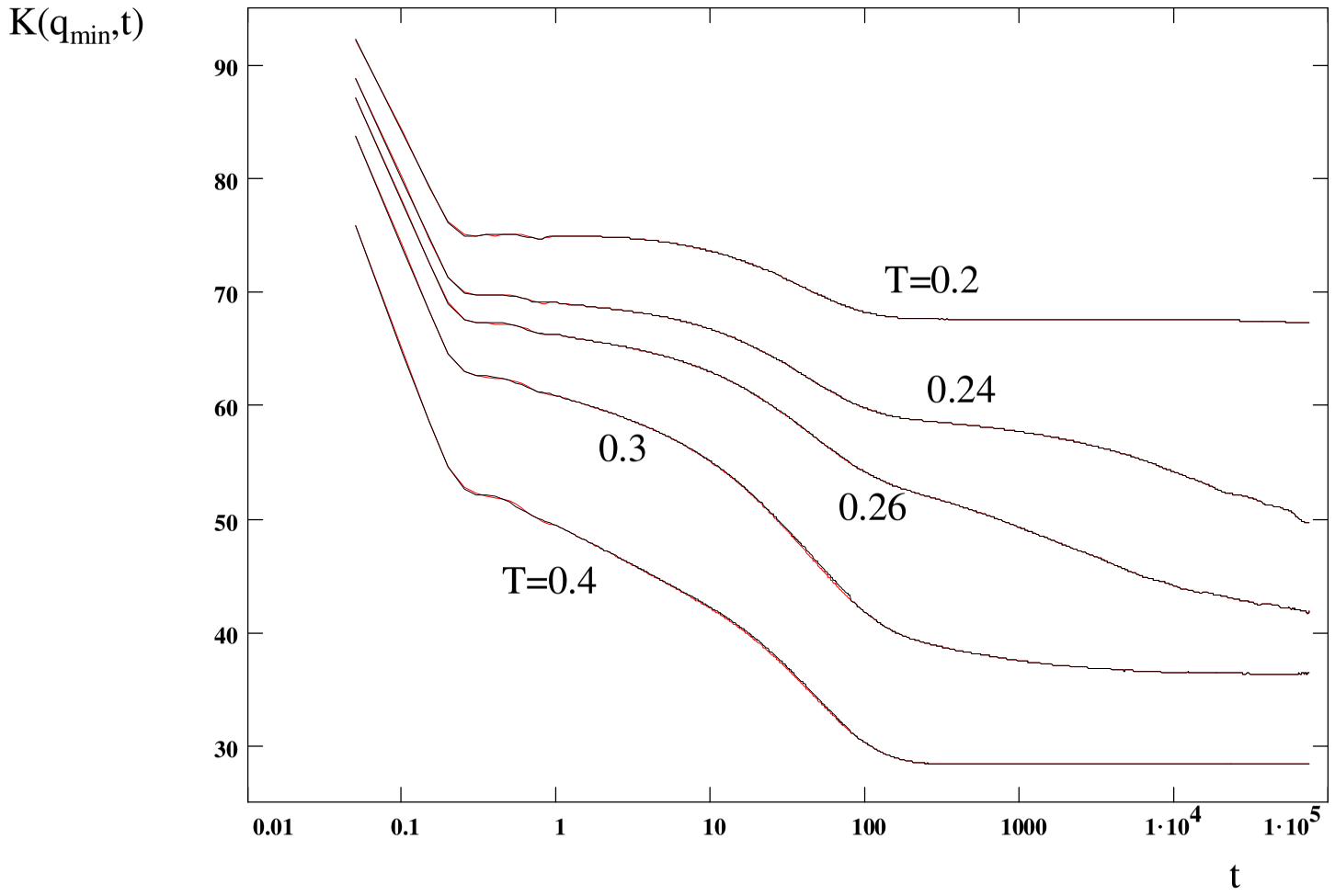
K(q_min,t)
90
80
70
60
50
40
30
0.01
0.1
1
10
100
1000
1·10^4
1·10^5
t
T=0.2
0.24
0.3
0.26
T=0.4

Fig. 1

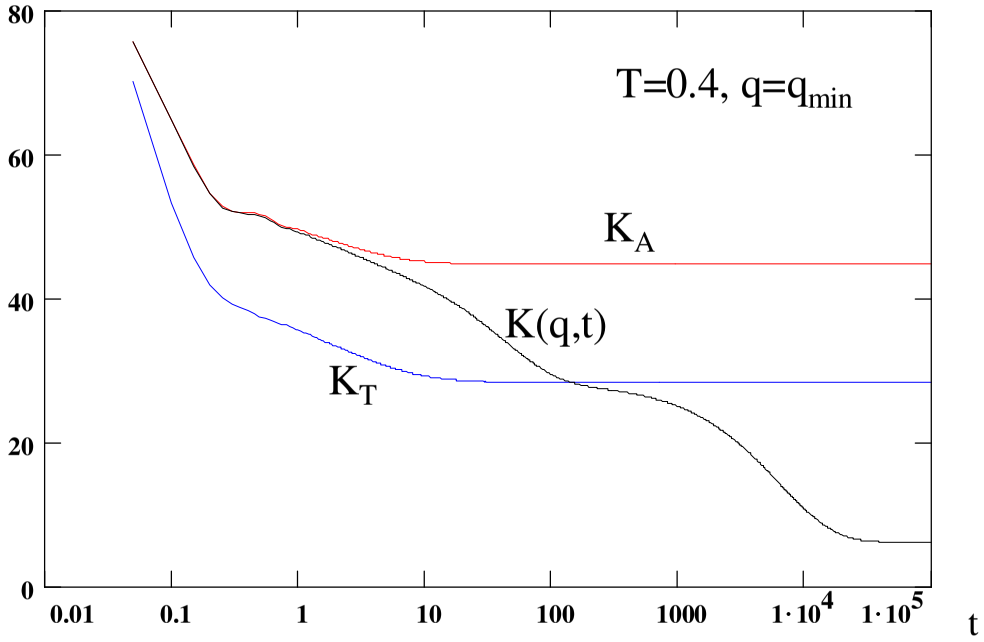
T=0.4, q=q_min
K_A
K(q,t)
K_T
80
60
40
20
0
0.01
0.1
1
10
100
1000
1·10^4
1·10^5
t

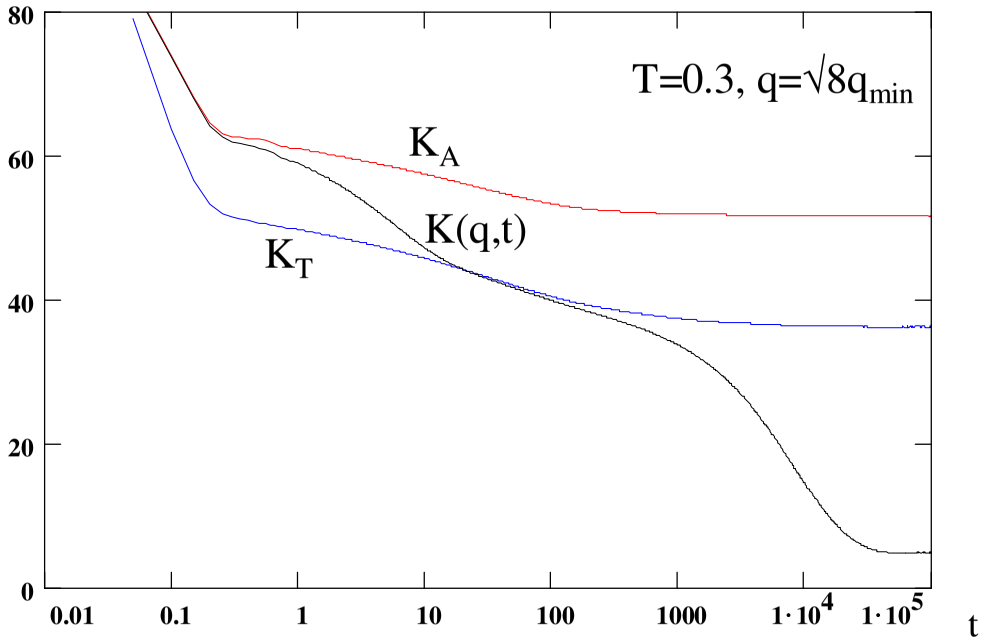
T=0.3, q=√8q_min
K_A
K(q,t)
K_T
80
60
40
20
0
0.01
0.1
1
10
100
1000
1·10^4
1·10^5
t

Fig. 2

Fig. 3

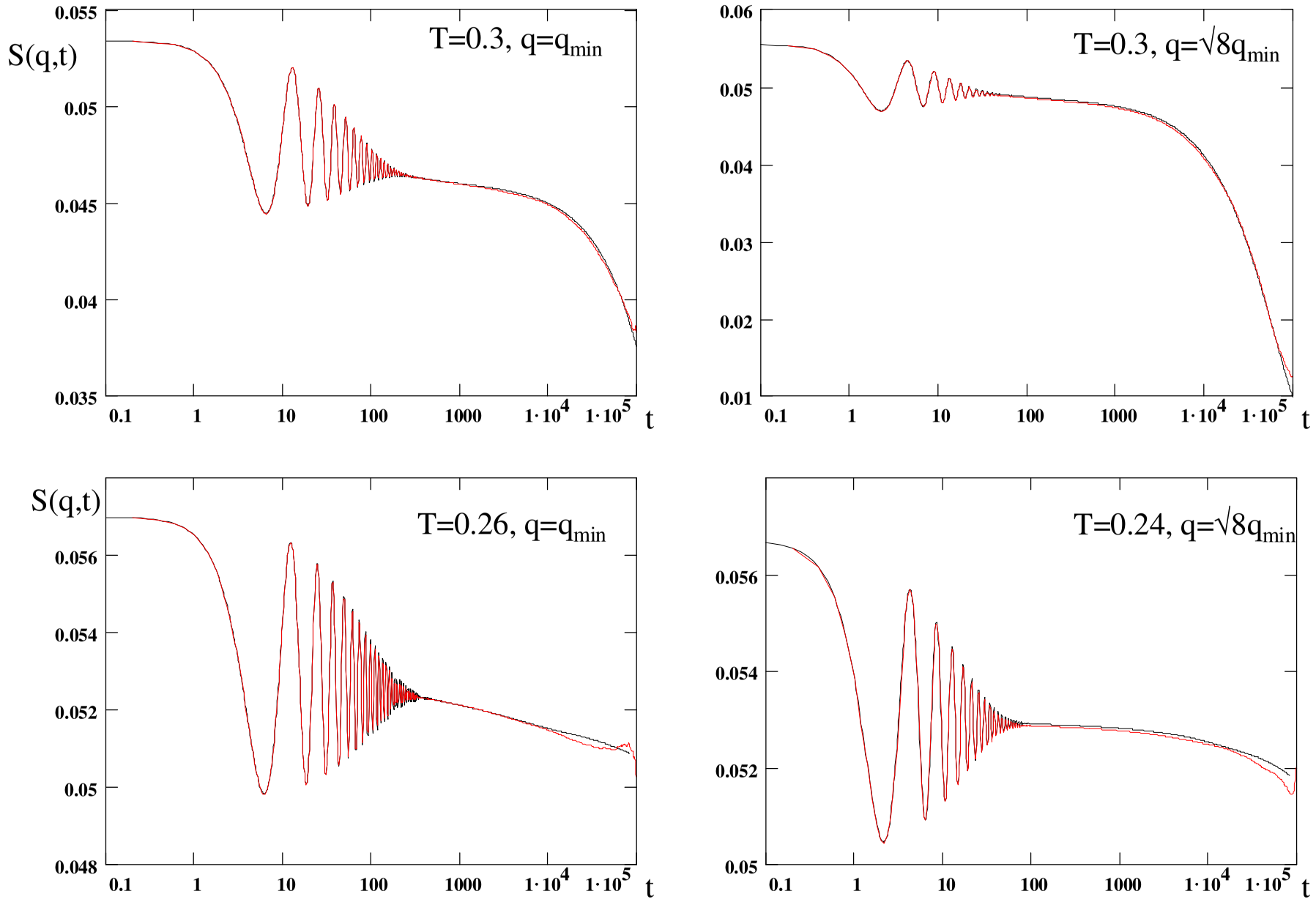
S(q,t)
T=0.3, q=q_min
0.055
0.05
0.045
0.04
0.035
0.1
1
10
100
1000
1·10^4
1·10^5
t
T=0.3, q=√8q_min
0.06
0.05
0.04
0.03
0.02
0.01
S(q,t)
T=0.26, q=q_min
0.056
0.054
0.052
0.05
0.048
T=0.24, q=√8q_min

Fig. 4 (a)

T=0.4

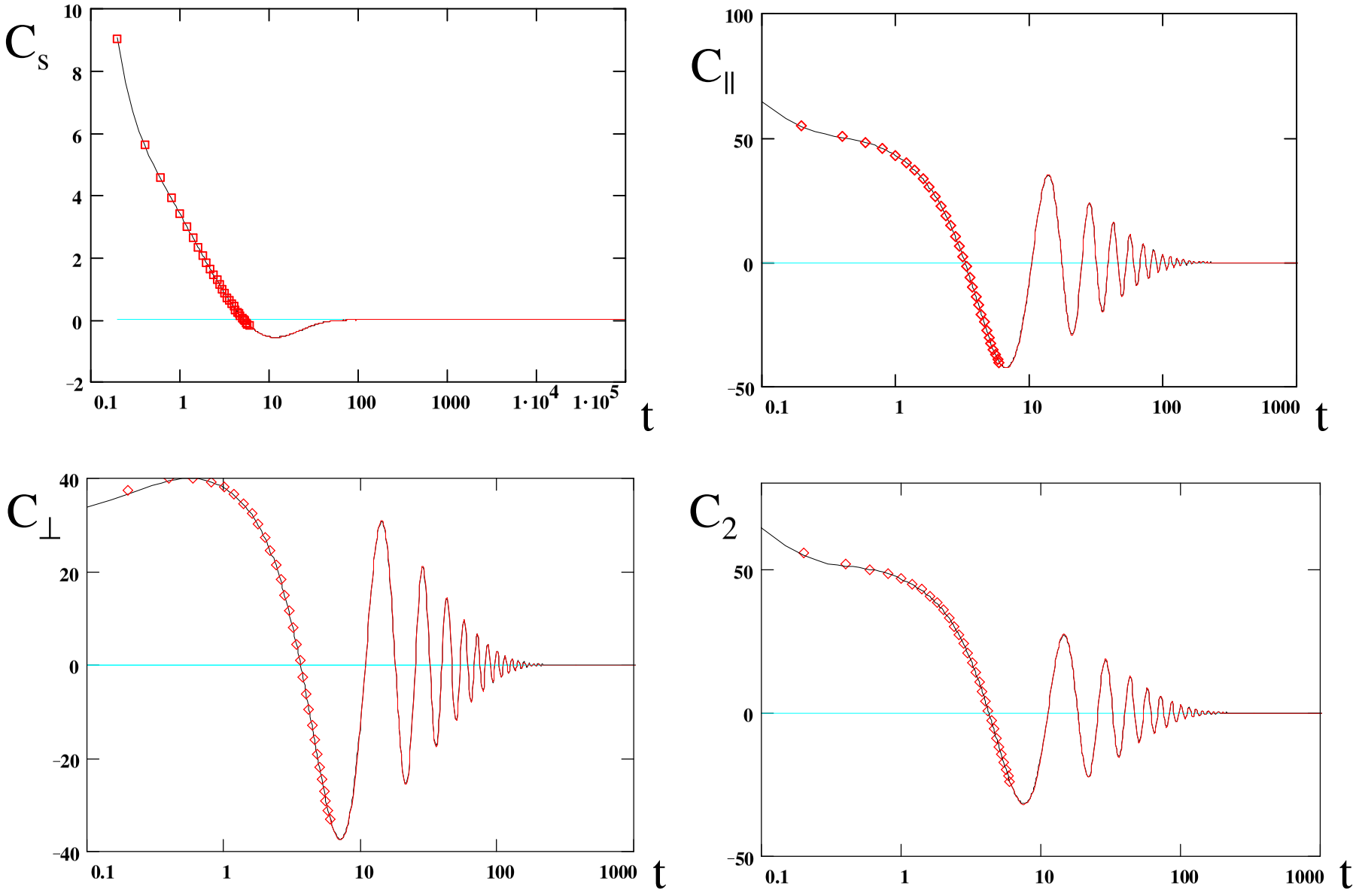
C_s
10
8
6
4
2
0
−2
0.1
1
10
100
1000
1·10^4
1·10^5
t
$C_{\|}$
100
50
0
−50
0.1
1
10
100
1000
t
$C_{\perp}$
40
20
0
−20
−40
0.1
1
10
100
1000
t
C_2
50
0
−50
0.1
1
10
100
1000
t

Fig. 4 (b)

T=0.3

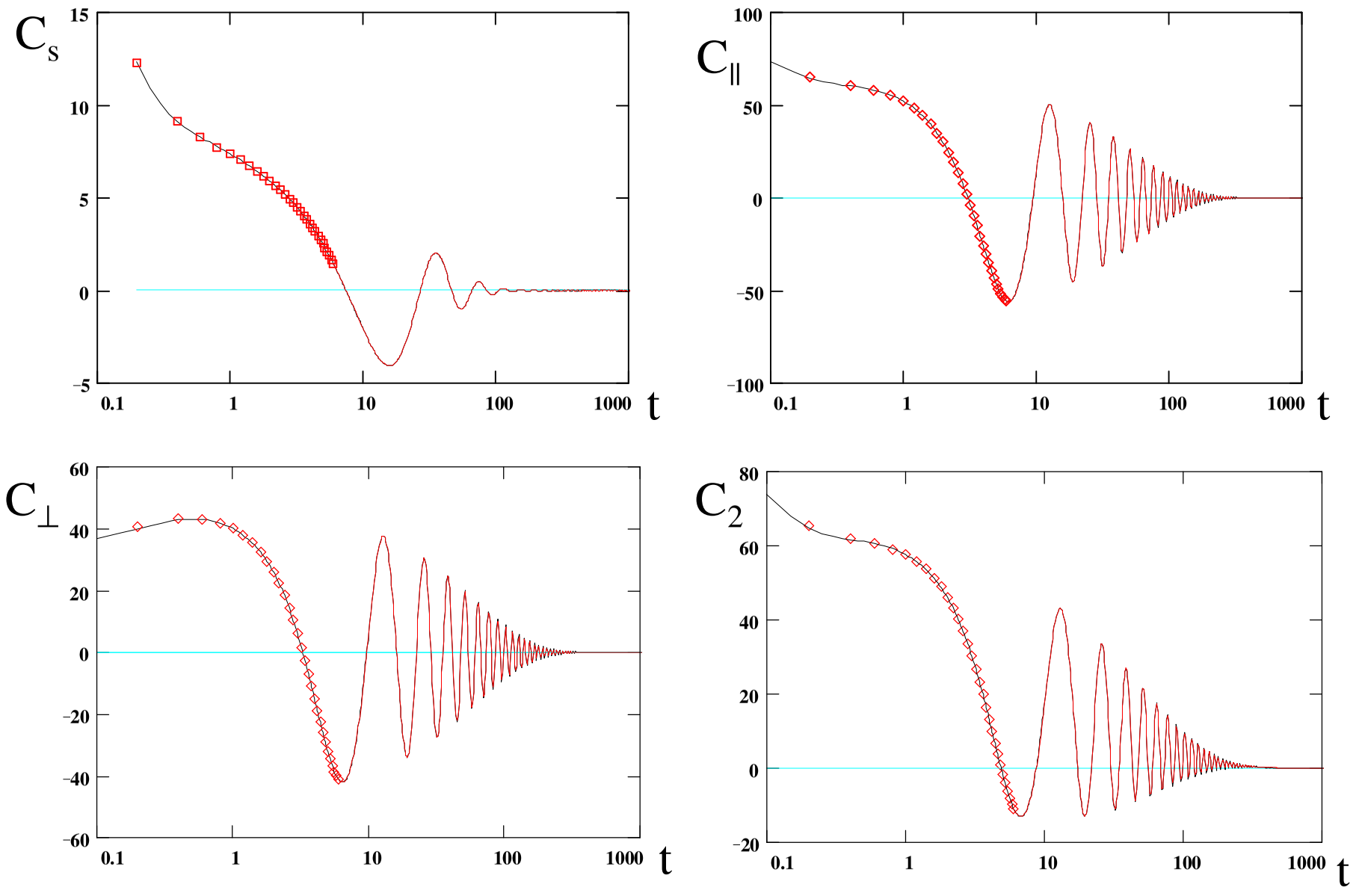
C_S
15
10
5
0
−5
0.1
1
10
100
1000
t
C_||
100
50
0
−50
−100
0.1
1
10
100
1000
t
C_⊥
60
40
20
0
−20
−40
−60
0.1
1
10
100
1000
t
C_2
80
60
40
20
0
−20
0.1
1
10
100
1000
t

Fig. 4 (c)

T=0.26

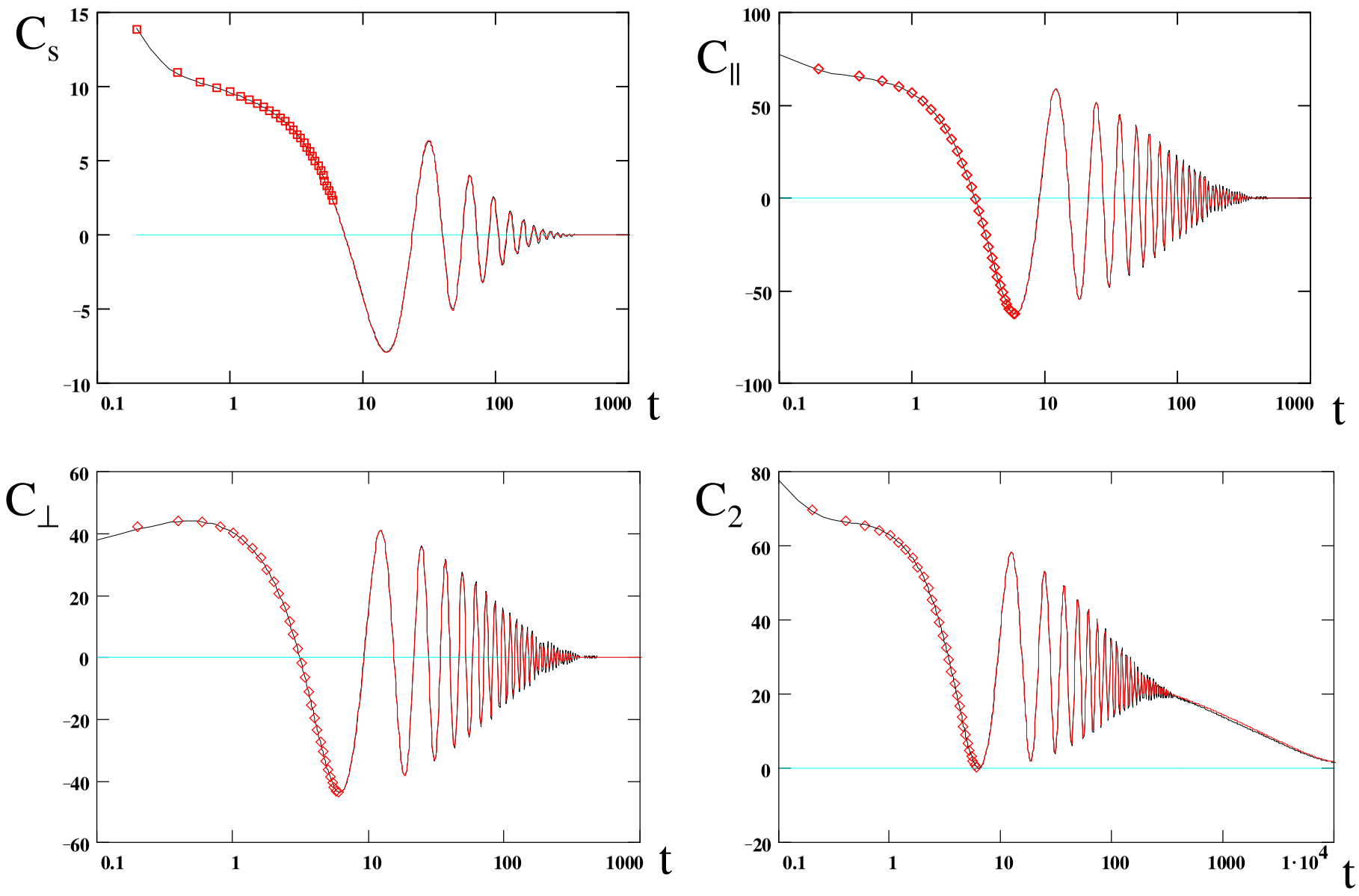
C_s
15
10
5
0
−5
−10
0.1
1
10
100
1000
t
$C_{\|}$
100
50
0
−50
−100
0.1
1
10
100
1000
t
$C_\perp$
60
40
20
0
−20
−40
−60
0.1
1
10
100
1000
t
C_2
80
60
40
20
0
−20
0.1
1
10
100
1000
$1\cdot10^4$
t

Fig. 4 (d)

T=0.24

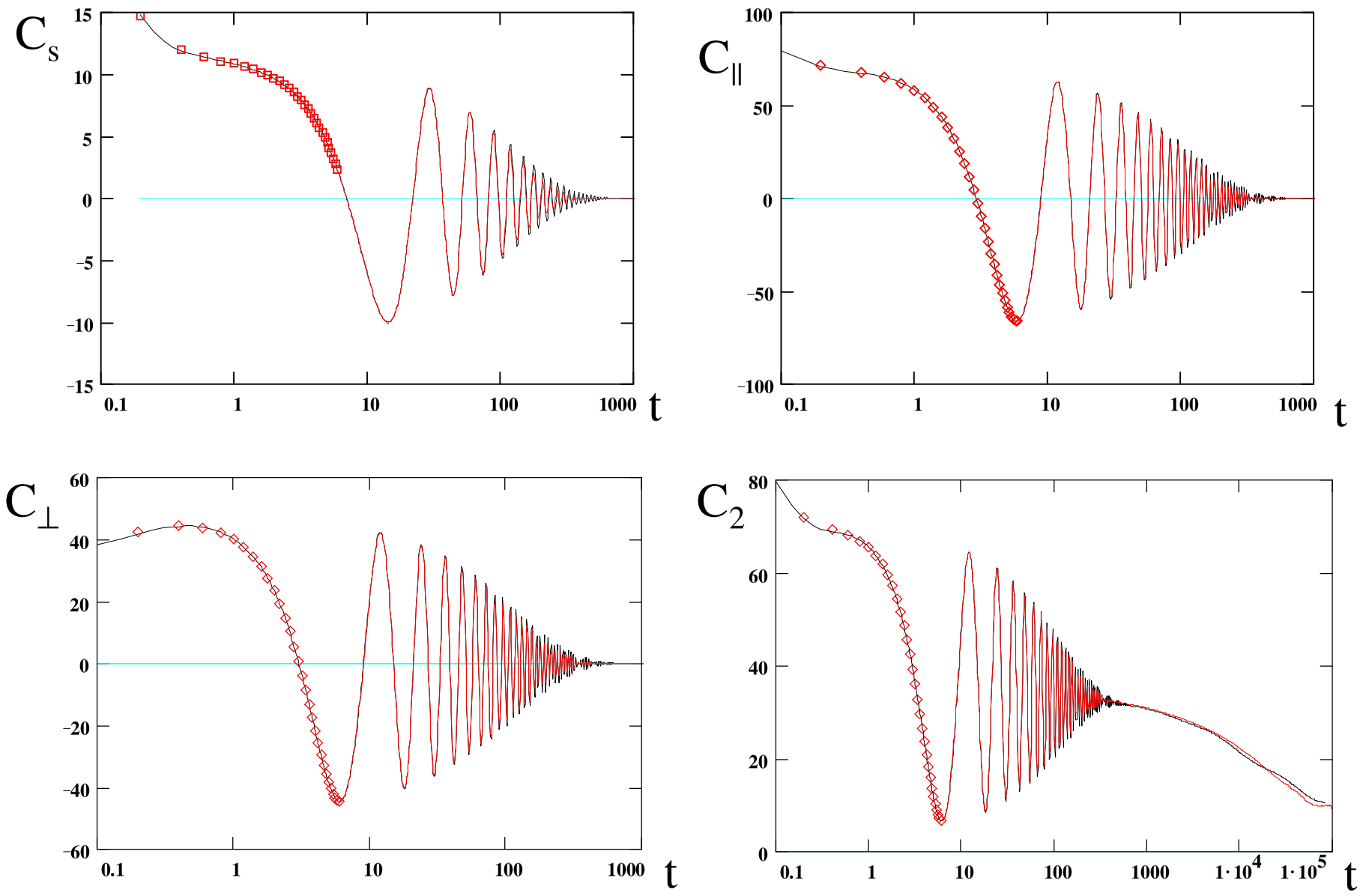
C_s
15
10
5
0
−5
−10
−15
0.1
1
10
100
1000
t
$C_{\|}$
100
50
0
−50
−100
0.1
1
10
100
1000
t
$C_\perp$
60
40
20
0
−20
−40
−60
0.1
1
10
100
1000
t
C_2
80
60
40
20
0
0.1
1
10
100
1000
$1\cdot10^4$
$1\cdot10^5$
t

Fig. 4 (e)

T=0.20

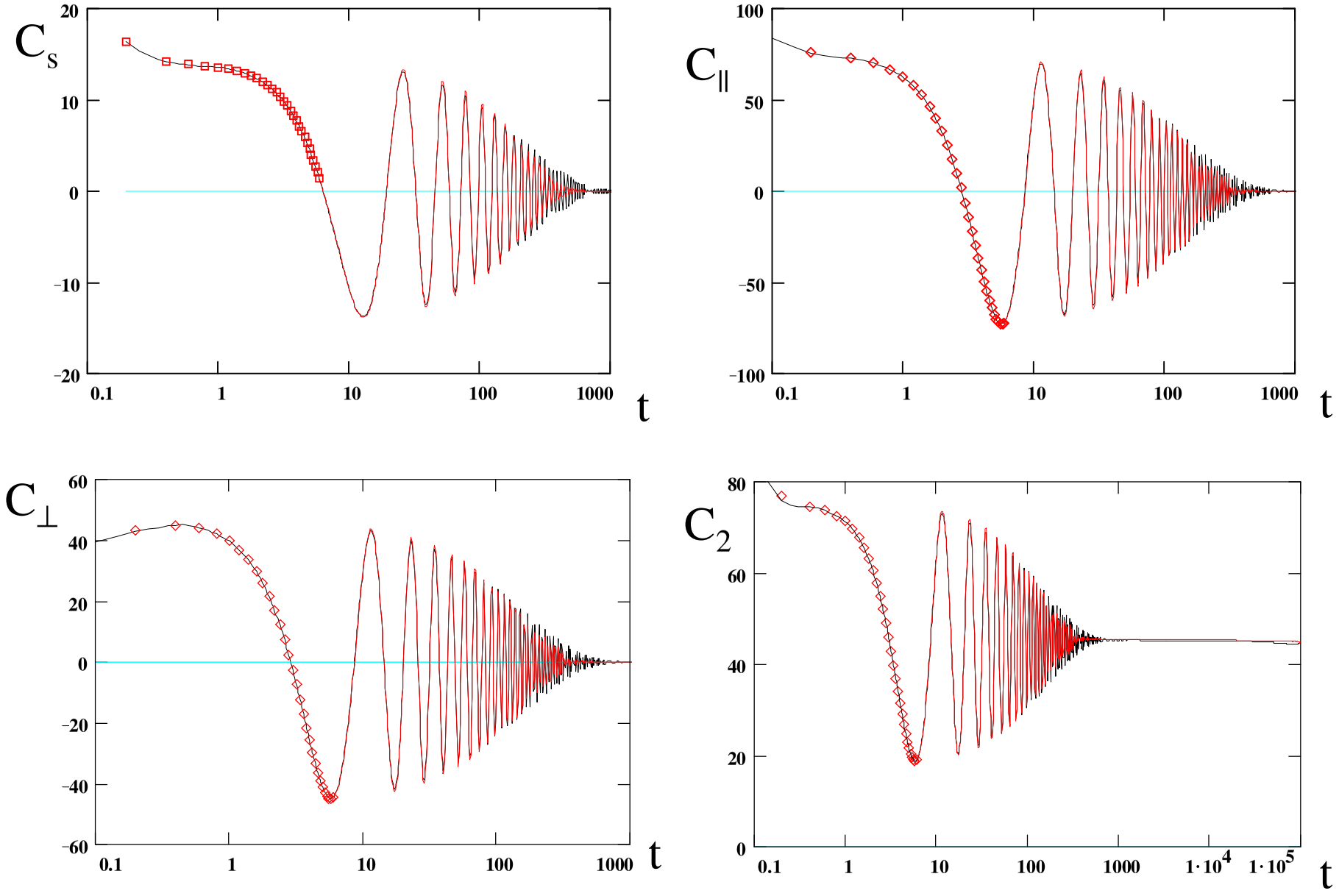
C_s
20
10
0
−10
−20
0.1
1
10
100
1000
t
$C_{\|}$
100
50
0
−50
−100
0.1
1
10
100
1000
t
$C_{\perp}$
60
40
20
0
−20
−40
−60
0.1
1
10
100
1000
t
C_2
80
60
40
20
0
0.1
1
10
100
1000
$1\cdot10^4$
$1\cdot10^5$
t

Fig. 5 (a)

$T=0.3,\ n_{q2}=8$

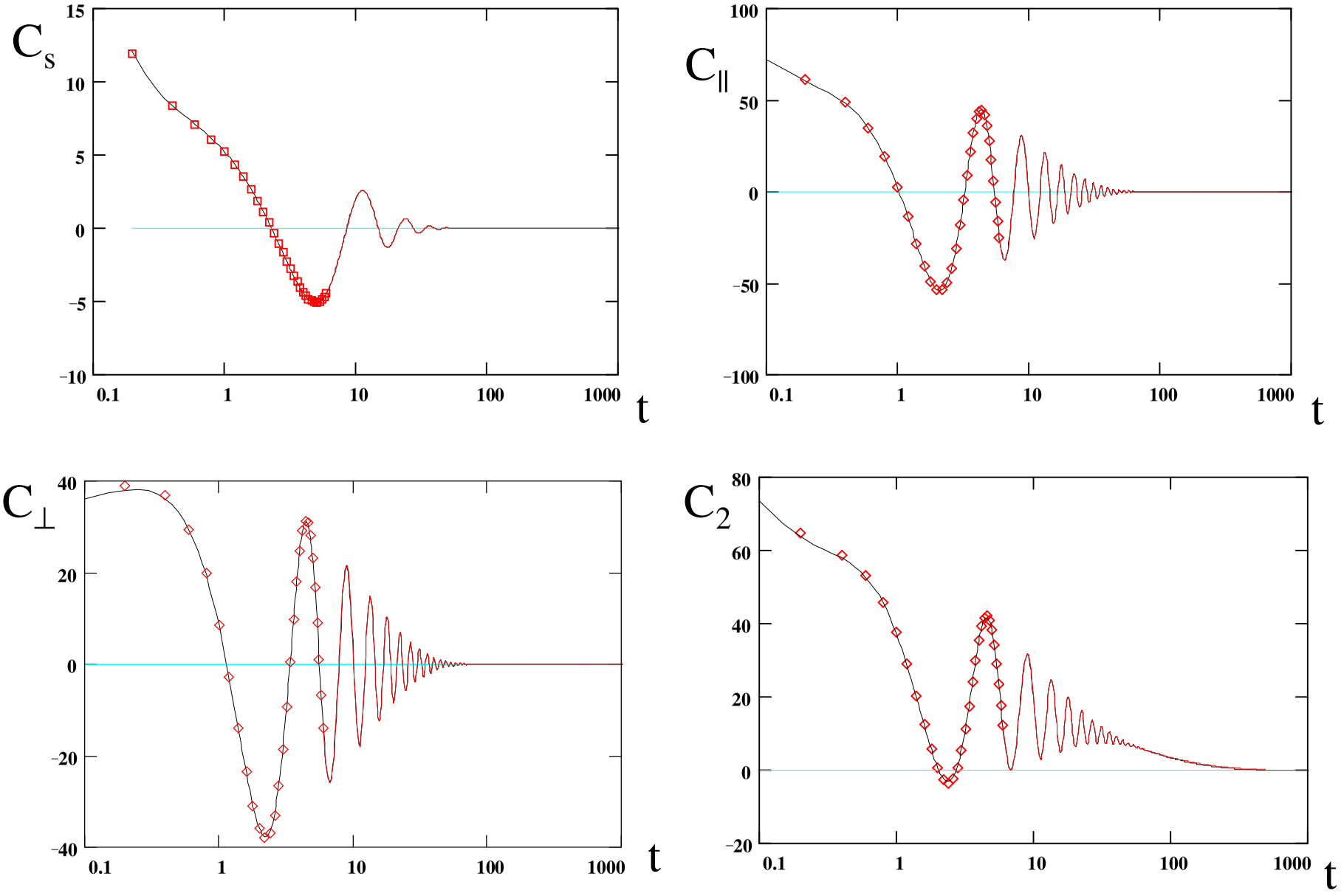

Fig. 5 (b)

$T=0.3,\ n_{q2}=32$

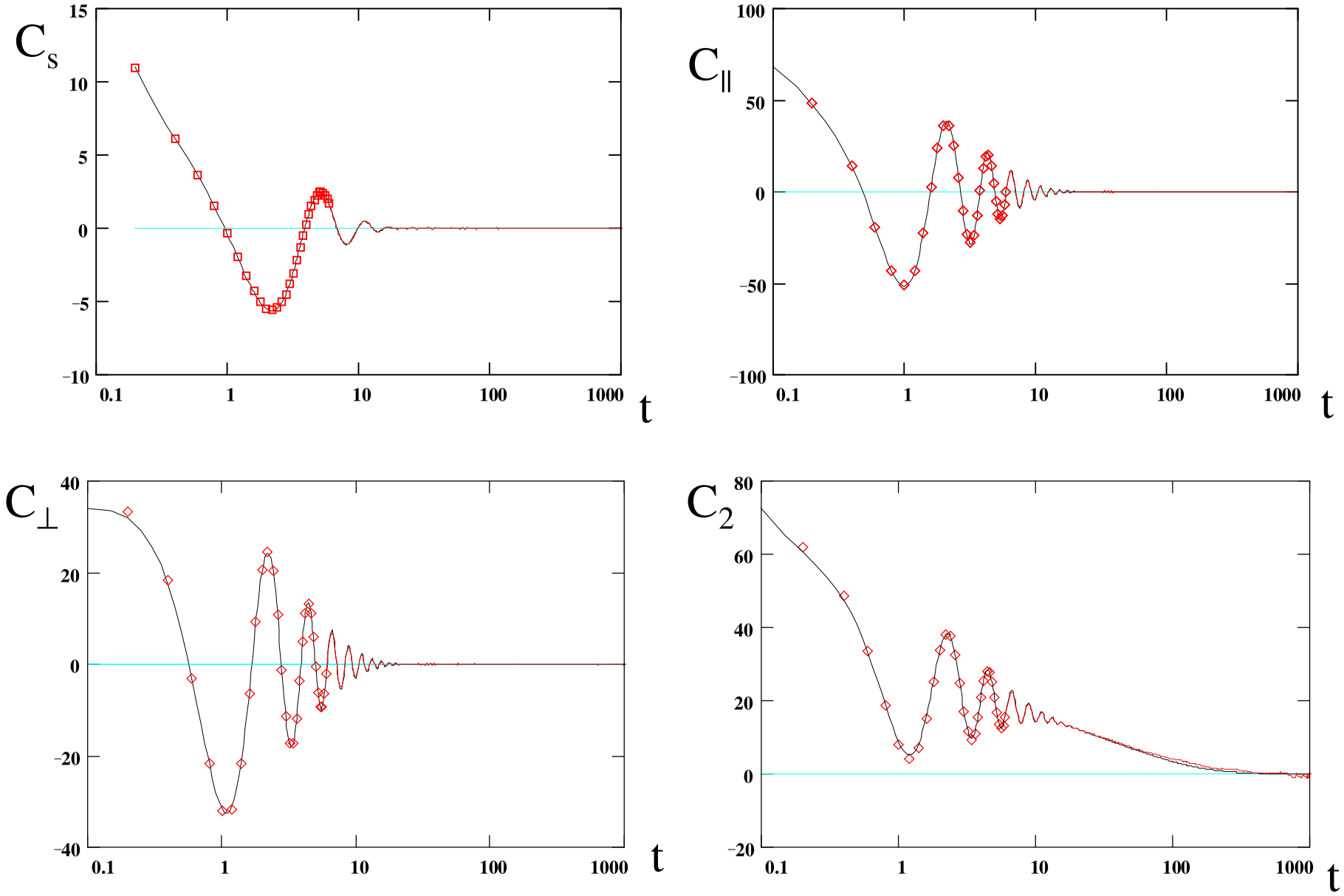

Fig. 5 (c)

$T=0.3,\ n_{q2}=64$

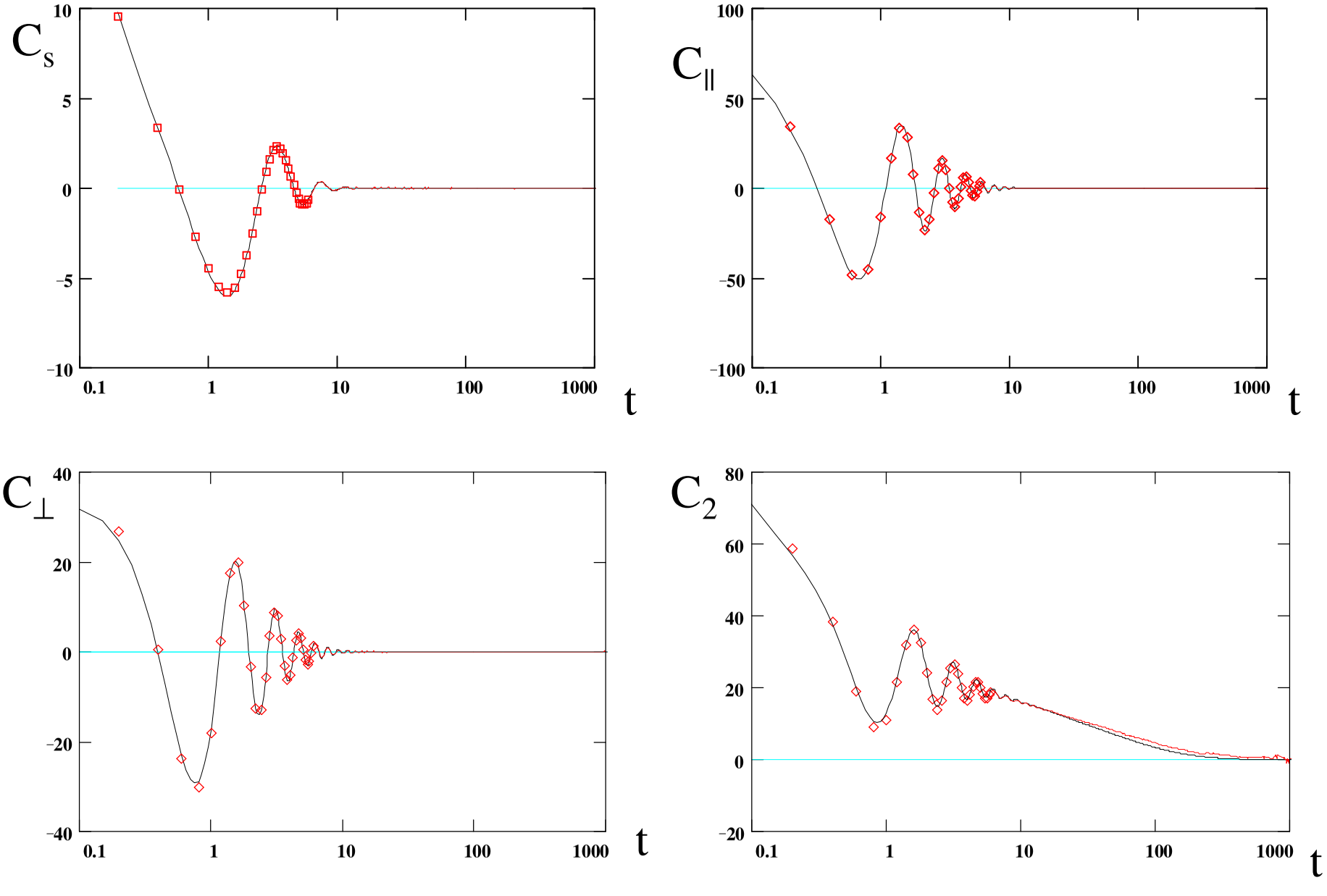

Fig. 6 (a)

$T=0.24,\ n_{q2}=8$

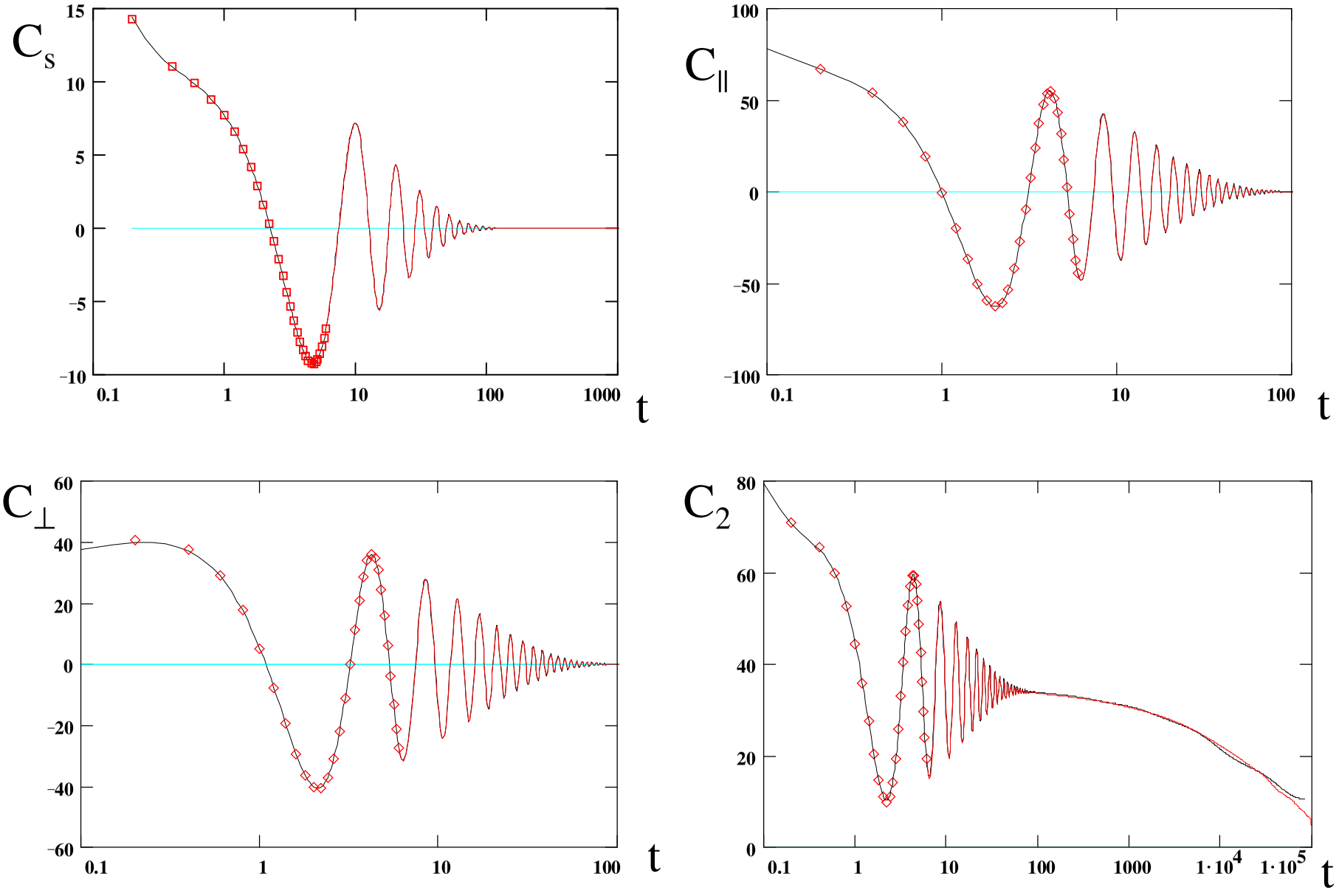

Fig. 6 (b)

$T=0.24,\ n_{q2}=32$

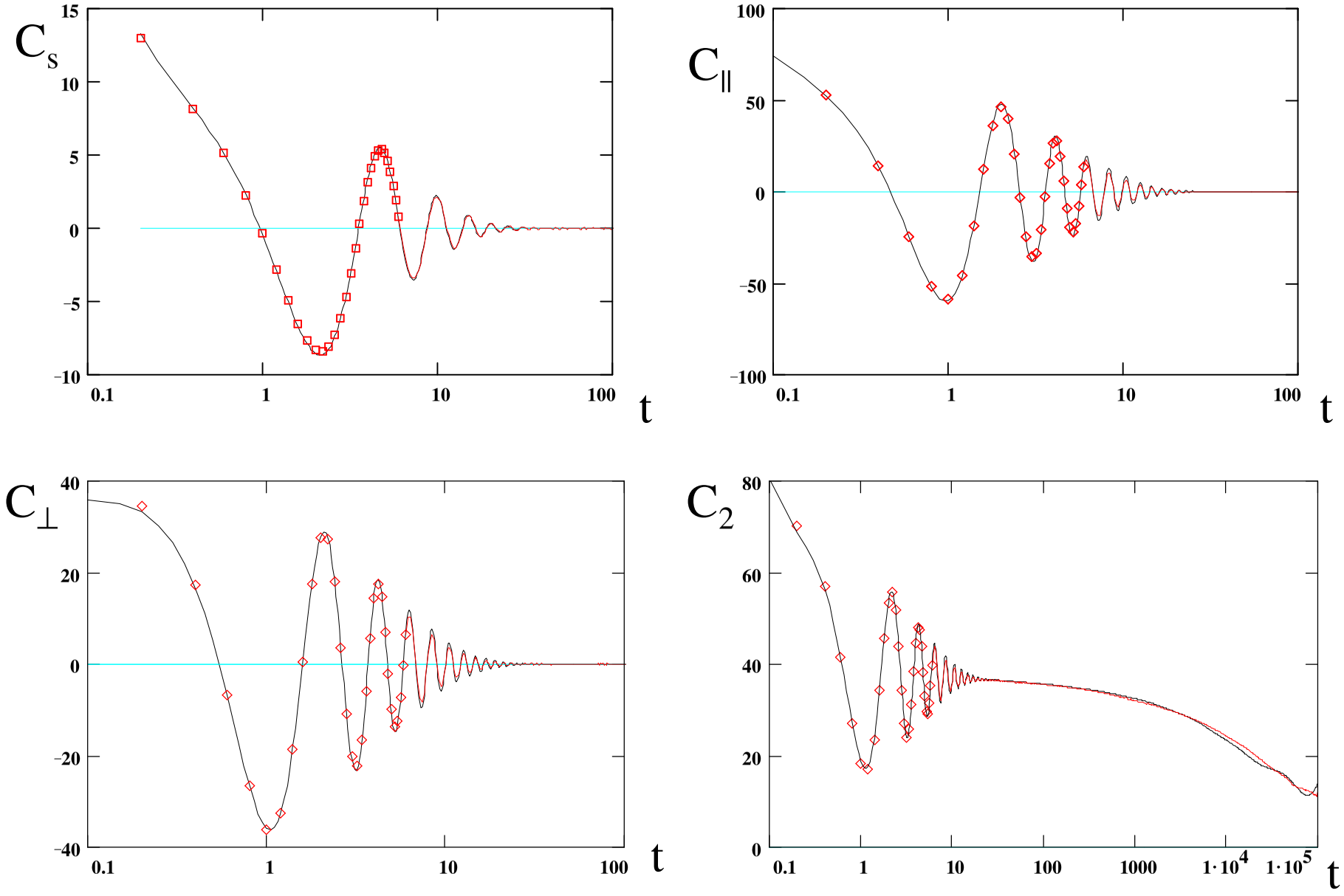

Fig. 6 (c)

$T=0.24,\ n_{q2}=64$

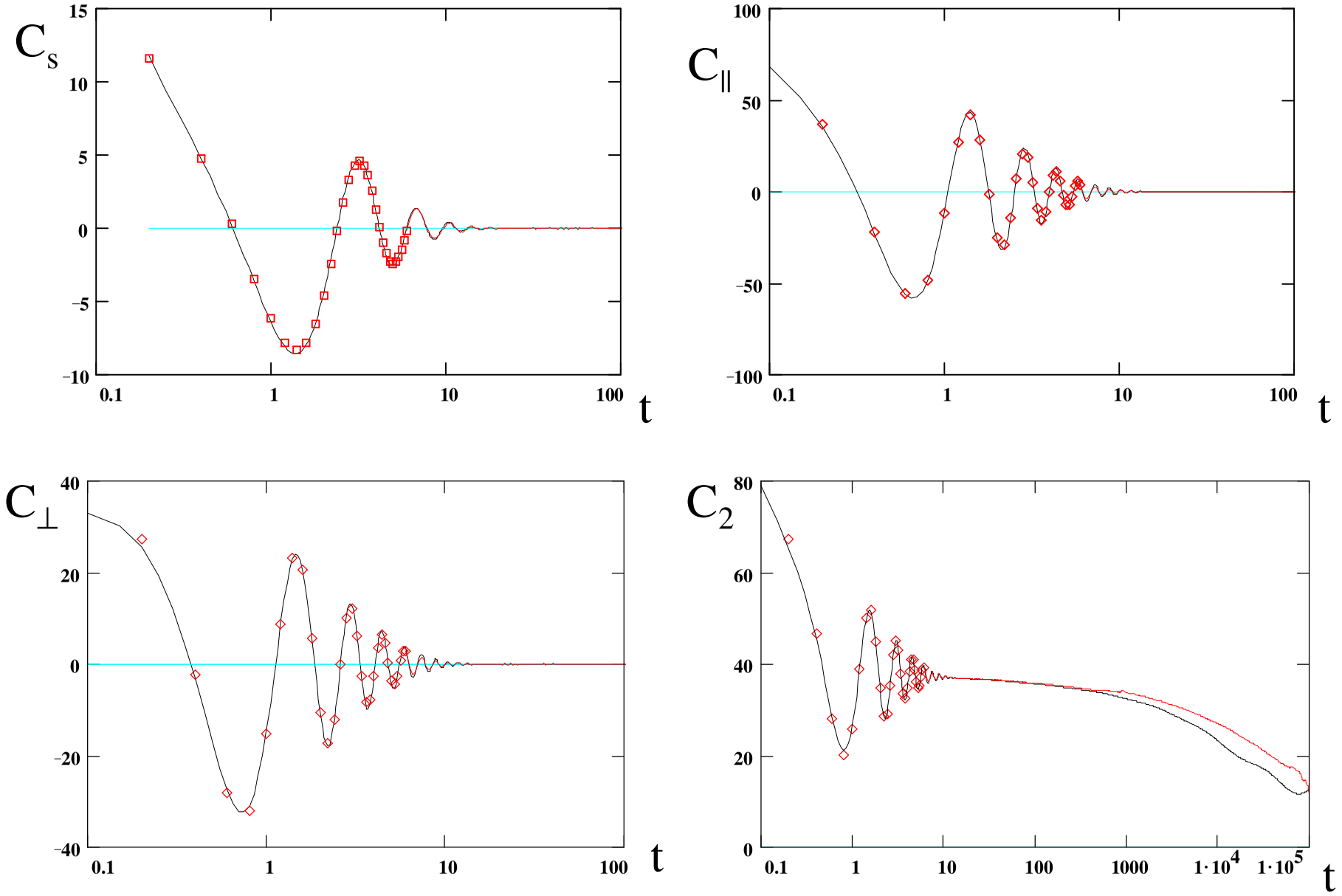

Fig. 7 (a)

$T=0.20,\ n_{q2}=8$

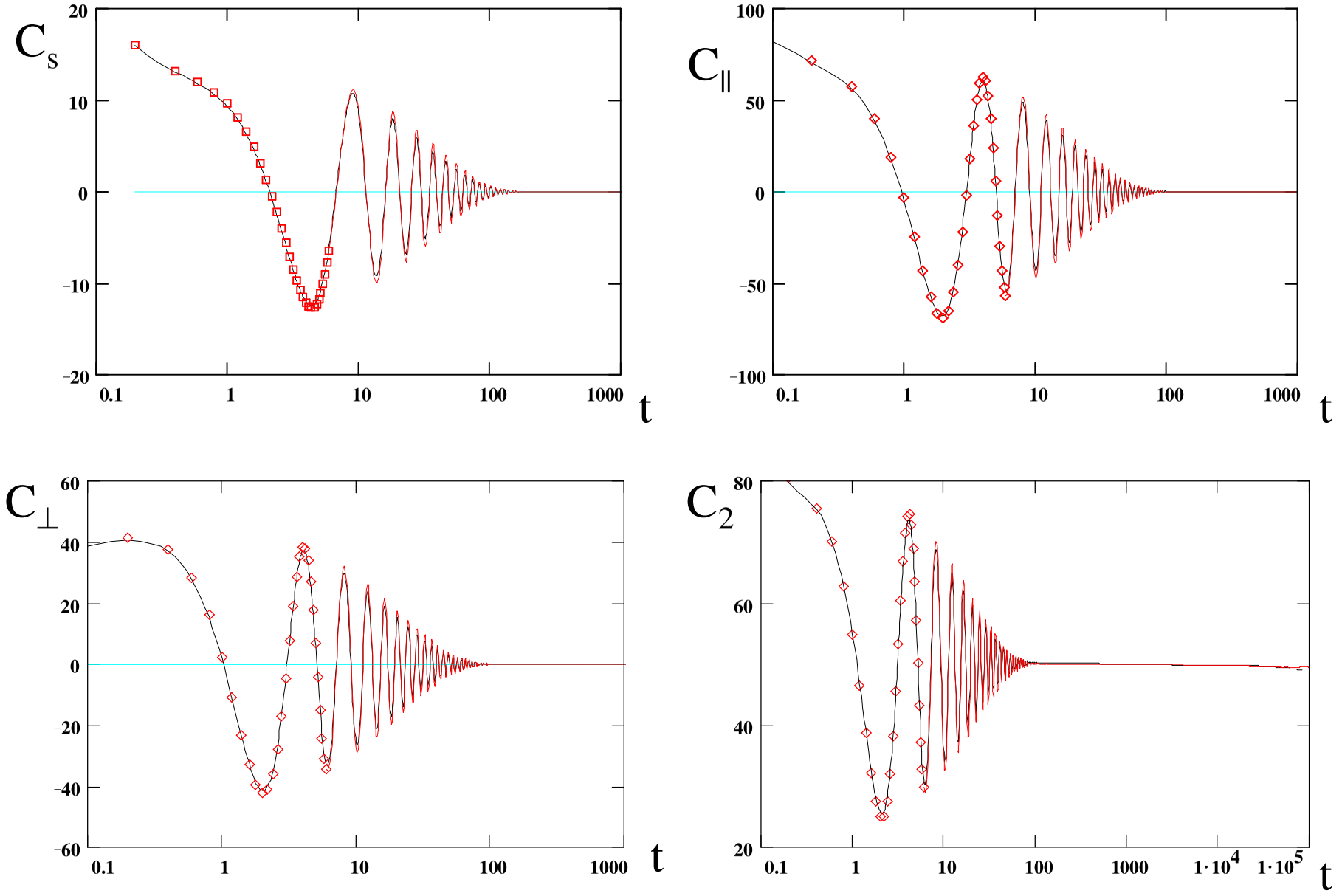

Fig. 7 (b)

$T=0.20,\ n_{q2}=32$

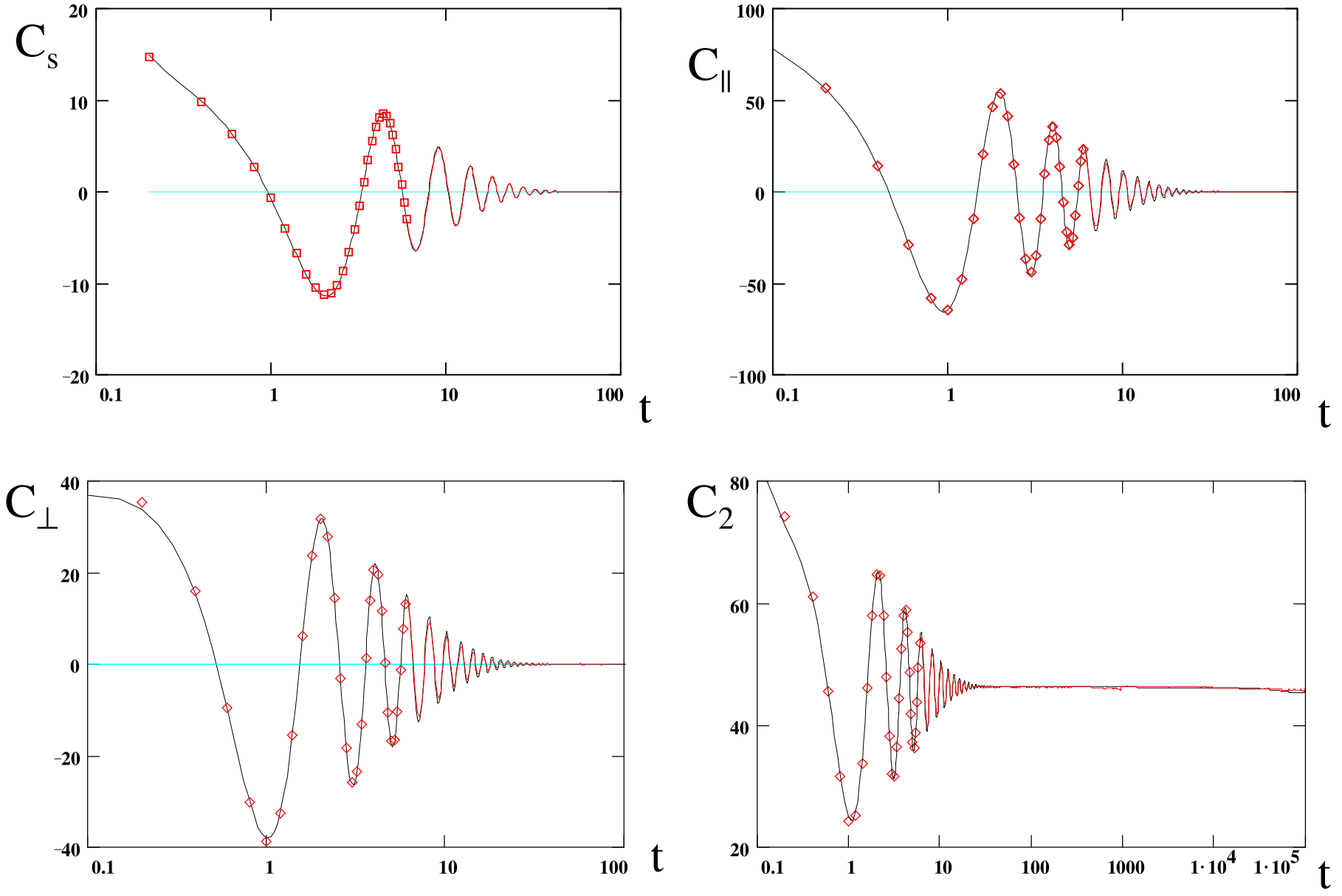

Fig. 7 (c)

$T=0.20,\ n_{q2}=64$

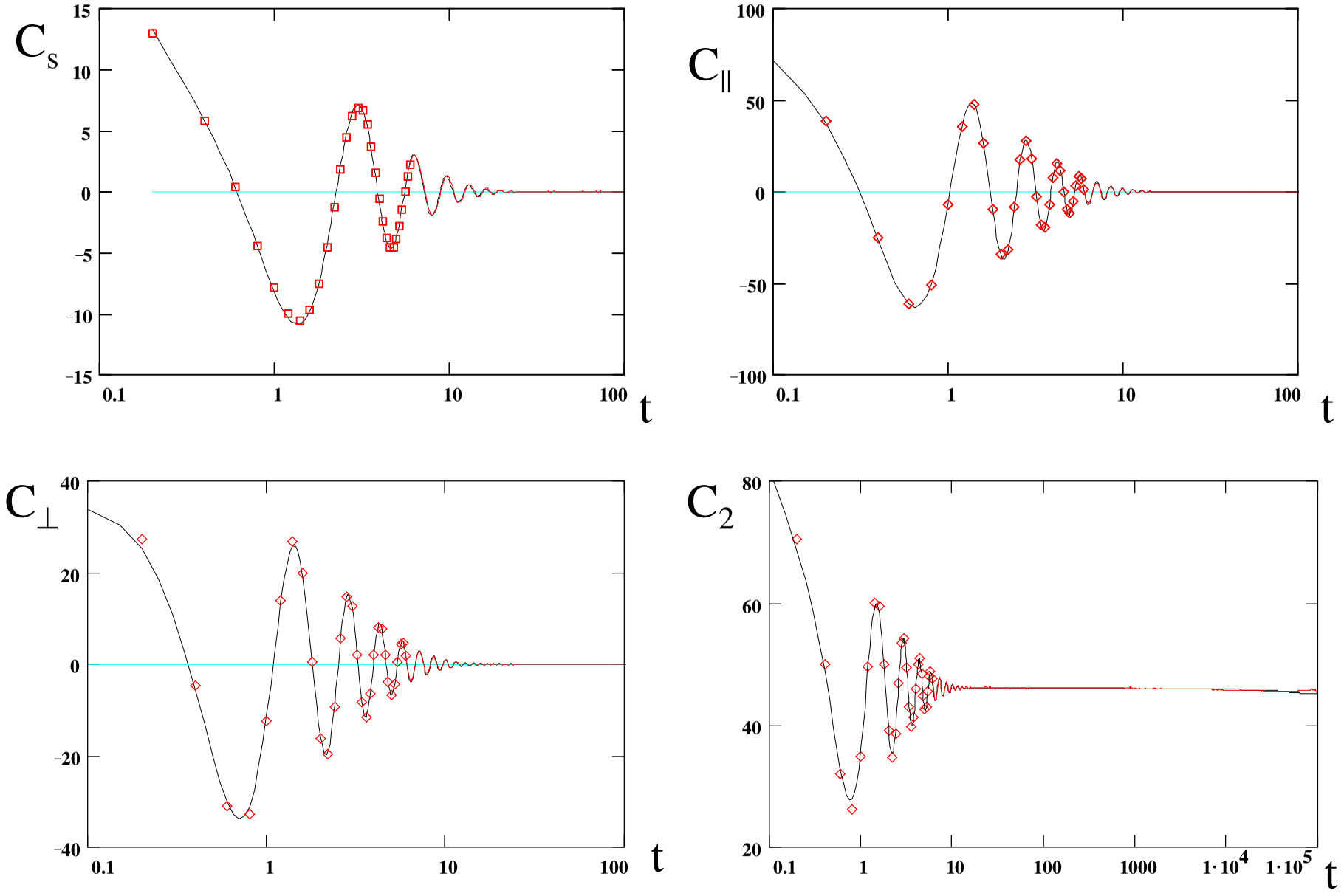

Fig. 8

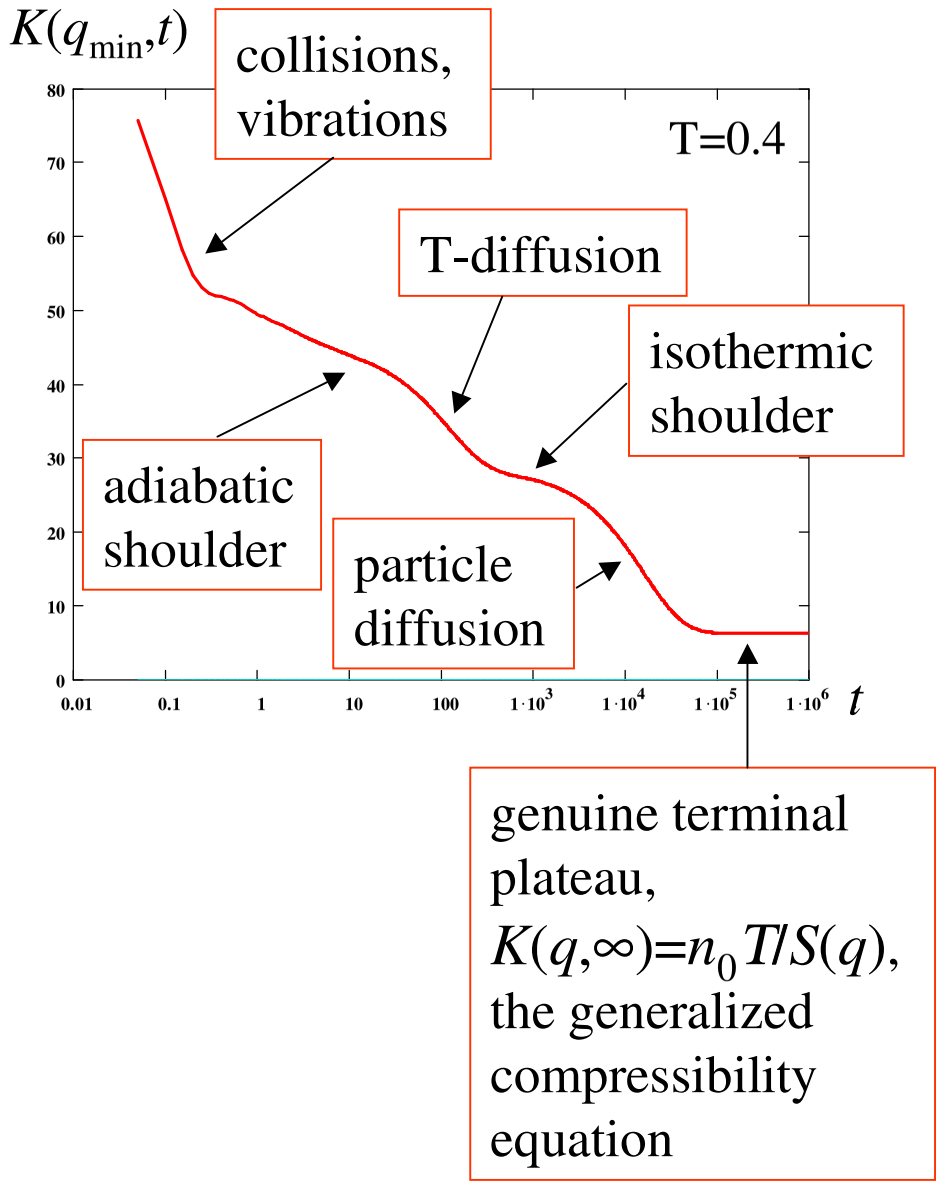
$K(q_{min},t)$
collisions, vibrations
T=0.4
T-diffusion
isothermic shoulder
adiabatic shoulder
particle diffusion
genuine terminal plateau, $K(q,\infty)=n_0 T/S(q)$, the generalized compressibility equation
80
70
60
50
40
30
20
10
0
0.01
0.1
1
10
100
$1\cdot10^3$
$1\cdot10^4$
$1\cdot10^5$
$1\cdot10^6$
t

Fig. 9

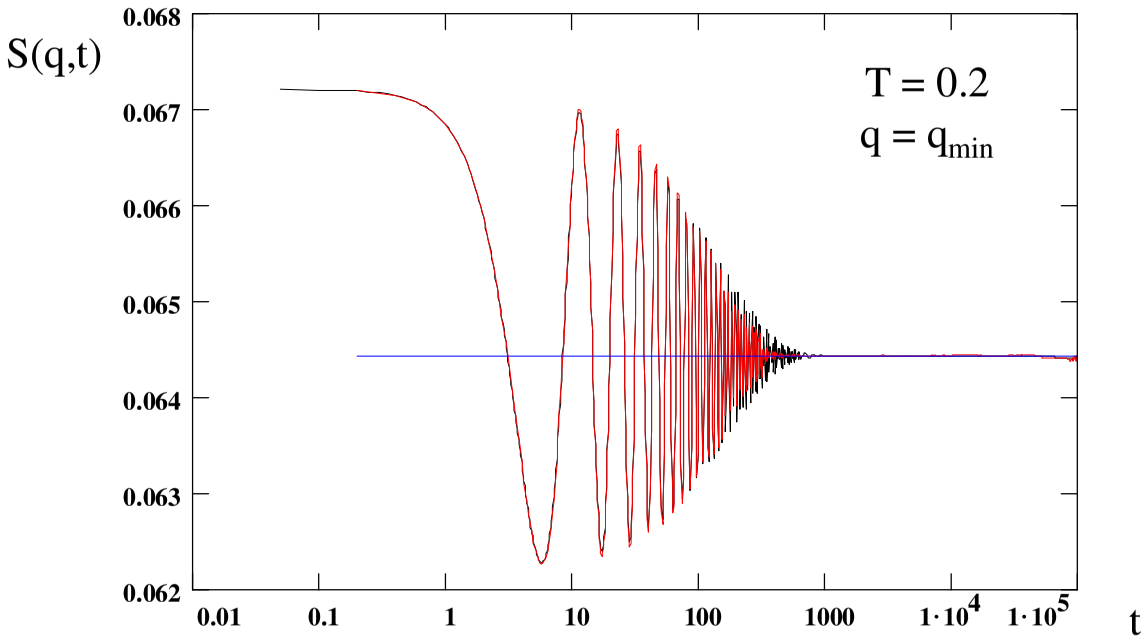
S(q,t)
0.068
0.067
0.066
0.065
0.064
0.063
0.062
T = 0.2
q = q_min
0.01
0.1
1
10
100
1000
1·10^4
1·10^5
t

Fig. 10

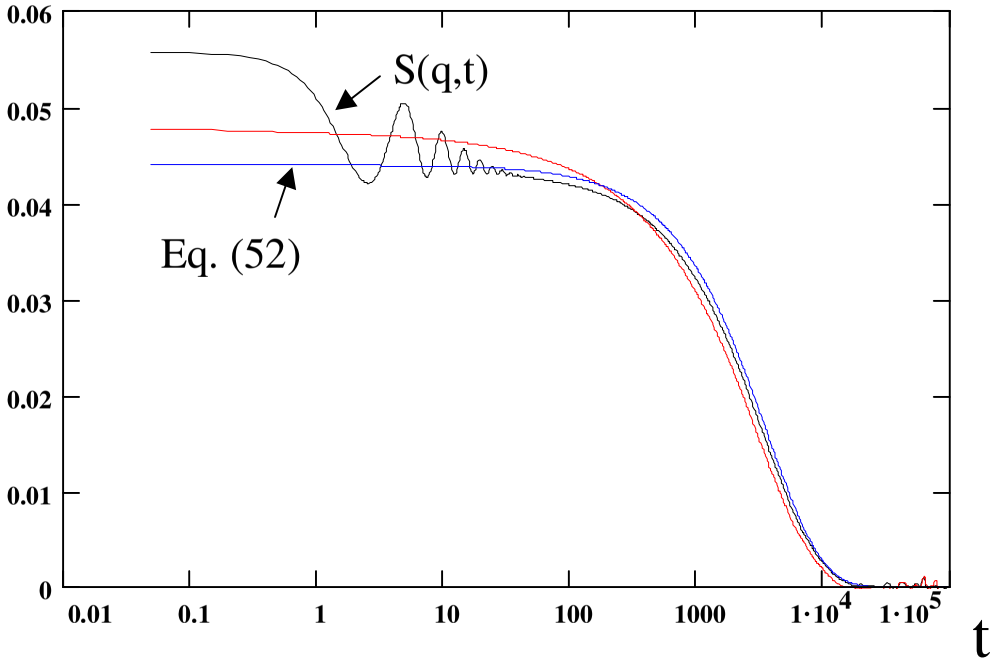
0.06
0.05
0.04
0.03
0.02
0.01
0
S(q,t)
Eq. (52)
0.01
0.1
1
10
100
1000
1·10^4
1·10^5
t